A UNITED STATES
DEPARTMENT OF
COMMERCE
PUBLICATION

NOAA Technical Report ERL 275–AOML 10

U.S. DEPARTMENT OF COMMERCE
NATIONAL OCEANIC AND ATMOSPHERIC ADMINISTRATION
Environmental Research Laboratories

Quantitative Marine Geomorphology
of the East Pacific Rise

DALE C. KRAUSE
PAUL J. GRIM
HENRY W. MENARD

BOULDER, COLO.
JULY 1973

NOAA TECHNICAL REPORT ERL 275–AOML 10

Quantitative Marine Geomorphology of the East Pacific Rise

DALE C. KRAUSE   Atlantic Oceanographic and Meteorological Laboratories, NOAA
PAUL J. GRIM   Environmental Data Service, NOAA
HENRY W. MENARD   Scripps Institution of Oceanography, University of California

NOTICE

TABLE OF CONTENTS

ABSTRACT

Marine geomorphology has been quantitatively studied on the East Pacific Rise at 35°S to test and extend earlier studies of the northeastern Pacific between Hawaii and California. Narrow-beam echo sounder profiles 110 km long were chosen to depict geomorphic provinces. Depth distributions are confirmed as generally normal. Departures from normal distribution can be explained on geological grounds. This new study was principally a test of earlier conclusions concerning distribution of sea-floor slopes. These conclusions have been confirmed. Log-log cumulative distributions of slopes are straight lines except for very steep slopes. Other unifying properties exist as well. These results confirm the conceptual model that the frequency of a slope is inversely proportional to its power, where the exponential factor lies between zero and +1. A basis therefore exists for classifying and mapping of sea-floor slopes using only one or two parameters. Our conclusion is that generalized processes exist which control the geomorphology of the entire East Pacific Rise in very specific and unified ways; thus, they yield geomorphic "laws" that control marine geomorphology.

QUANTITATIVE MARINE GEOMORPHOLOGY
OF THE EAST PACIFIC RISE

Dale C. Krause
Atlantic Oceanographic and Meteorological Laboratories, NOAA

Paul J. Grim
Environmental Data Service, NOAA

Henry W. Menard
Scripps Institution of Oceanography
University of California

1. INTRODUCTION

Despite the great advances in the knowledge of sea-floor tectonic processes during the last few years, our knowledge of the processes and laws controlling the detailed geomorphology of the rough sea floor is very limited. One fruitful method of study is to quantify the problem by applying statistical techniques to representative bathymetric profiles. The measures can then be used to infer geomorphic processes, either known or as yet unidentified.

Quantitative geomorphic studies have been made of the East Pacific Rise at 35°S as a test of unique results obtained from an earlier study of the Northwest Pacific sea floor (Krause and Menard, 1965, and unpublished results). The earlier study showed that (1) the depth frequency of a 111-km bathymetric profile tends toward a Gaussian distribution, and (2) the slope distribution of such a profile is strongly controlled and can be simply described by a single parameter. The conclusions of the earlier study have been confirmed for the South Pacific and are reported herein with the confirming results. A conceptual model is developed to explain the frequency distribution of sea-floor slopes.

1.1 Comparison of Conditions

The two studies are similar and are based on essentially similar assumptions, but the newer study incorporates several improvements in techniques. The older study used units of fathoms (fm) and nautical miles (n miles) and is so reported here. The old units are kept because the statistical measures are tied to them in that study. The newer study is in metric units and is so reported. The statistical measures and ratios are quite comparable (1 fm = 1.829 m, 1 n miles = 1.852 km).

1.2 Northeast Pacific Study

In the study of Krause and Menard (1965), fifteen 60 n mile long profiles of the northeast Pacific Ocean were chosen to represent different bathymetric provinces (figs. 1, 2, and 3). These profiles are perpendicular to the regional trend (except the one over an abyssal plain where trend is unimportant). The profiles were recorded on conventional 12-kHz Edo UQN/1B depth recorders (30° transducer sound cone angle between half-power points) on ships of the Scripps Institution of Oceanography (University of California) and the U. S. Naval Undersea Research and Development Center (formerly the U. S. Naval Electronics Laboratory). Depths were read at 3-min intervals, which represent a distance of 0.484 to 0.632 n miles (0.897 to 1.171 km), depending upon the ship's speed (table 1). Depths were read to the nearest 5 fm (9.1 m). The main features of the recorded profiles are shown on the plotted profiles (figs. 2 and 3), and the data can therefore be used with confidence in the analyses (Krause and Menard, 1965).
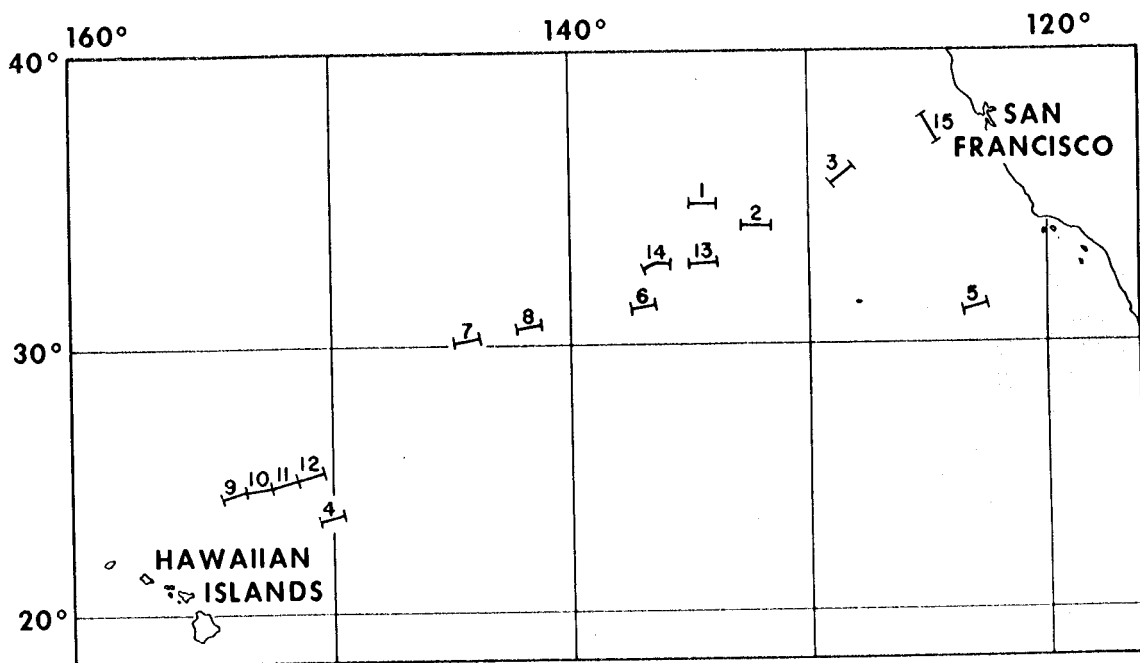
Figure 1. *Location of bathymetric profiles in northeastern Pacific Ocean (from Krause and Menard, 1965).*

Figure 3. Bathymetric profiles 9 to 15, northeastern Pacific Ocean (from Krause and Menard, 1965).

Figure 2. Bathymetric profiles 1 to 8, NE Pacific Ocean. Units in 3-min intervals along profile (distance: 111 km, 60 n miles). See Table 1. Dashed lines show division of profile into abyssal hills (from Krause and Menard, 1965).

-3-

1.3 South Pacific Study

Twenty-six 111 to 222 km long profiles over the East Pacific Rise at 35°S are chosen to test the North Pacific results (figs. 4, 5, 6, and table 1). They represent diverse bathymetric provinces (see section 5.1 Frequency Distribution of Depths). Most of the profiles are chosen to be 111 km (60 n miles) long because longer profiles included more diverse topography, and shorter ones are undesirable from a statistical aspect. The six 222-km profiles are examined to see the effect of long profiles. These long profiles — 9*, 12*, 15*, 20*, 23*, and 26* — are marked with an asterisk. By experimental design, all profiles are perpendicular to the bathymetric trends. They are located over the crest and on the eastern flank of the East Pacific Rise. The profiles were recorded with the 20-kHz General Electric narrow-beam echo sounder (3.5° between half-power points) on the NOAA Ship *Oceanographer*. Depths were measured at 2.5-min intervals (representing 1.00 to 1.31 km, depending on speed), as well as at significant peaks and troughs within the standard intervals. Depths were read to the nearest fathom, corrected for sound velocity (Matthews, 1939), and converted to the nearest meter. The North Pacific depths are not corrected for sound velocity. The sound velocity correction in the North Pacific amounts to 45 to 100 fm, depending on depth. This does not significantly affect the slope distribution and only marginally affects the depth distributions in their dispersion.
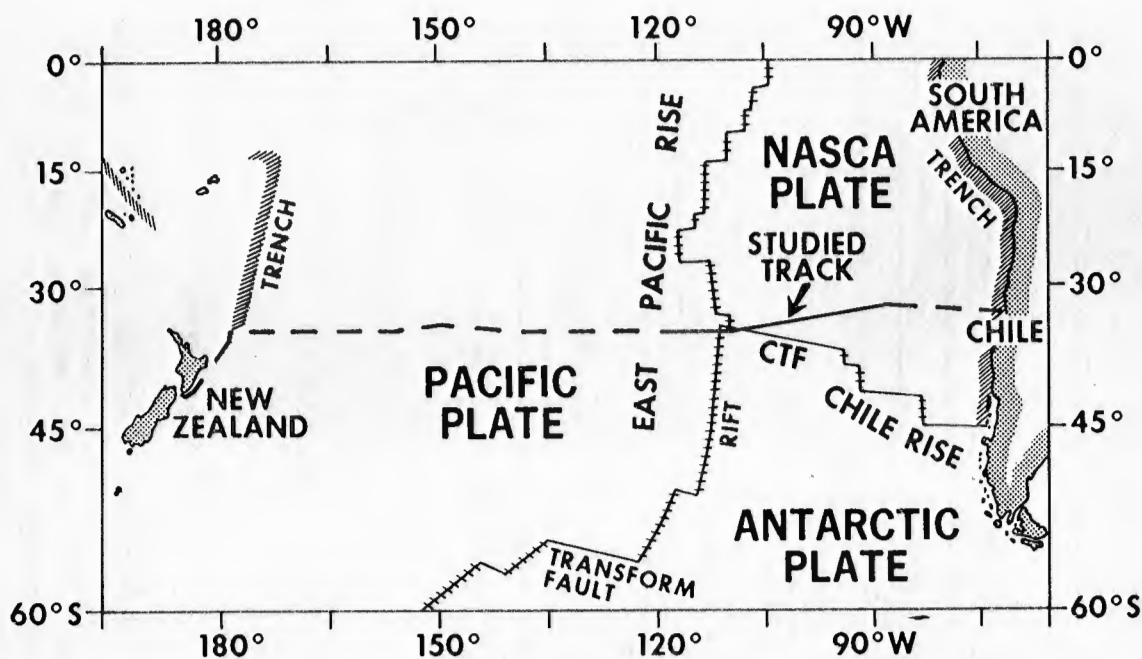
Figure 4. *Crossing of South Pacific by NOAA Ship OCEANOGRAPHER in October 1967. Solid line shows track relative to tectonic plates, rift of East Pacific Rise and Chile transform fault (CTF).*
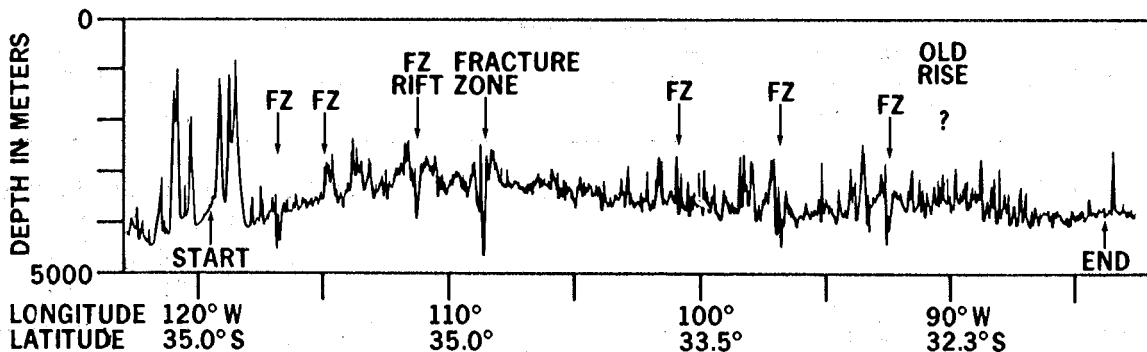
Figure 5. *Bathymetric profile along studied OCEANOGRAPHER track, South Pacific, indicating identified fracture zones (FZ), main rift of East Pacific Rise, and an inferred inactive rise. Vertical exaggeration is 200 times.*
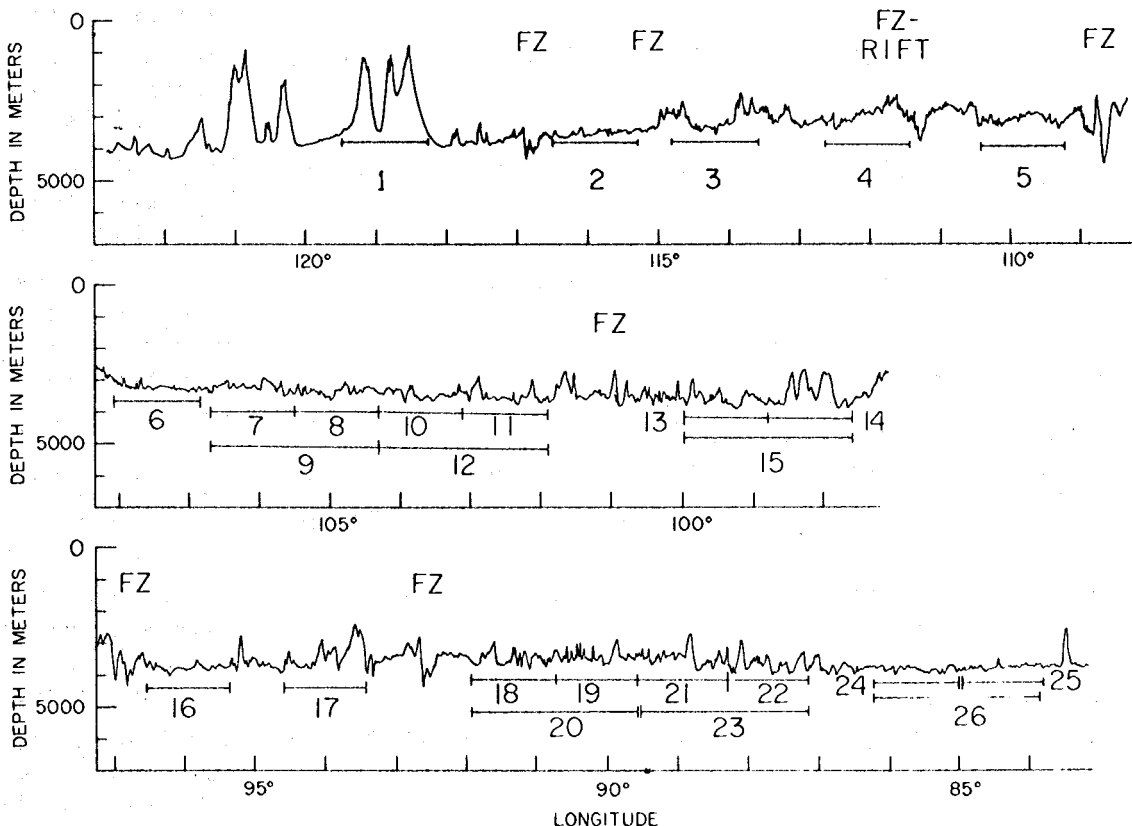
Figure 6. *Location of subprofiles of detailed study along OCEANOGRAPHER profile, South Pacific (see also fig. 5). Profiles are 111 km long except for six profiles 222 km long. Vertical exaggeration is 50 times.*

Table 1. Profile Data, North Pacific[1]

Profile	Length of 3-min Interval (n mile)	No. of Intervals	Ship	Date	Character
1	0.566	106	*Baird*	11 Aug 53	North of Murray Fracture Zone, large hills, irregular relief
2	0.545	110	*Baird*	13 Aug 53	North of Murray Fracture Zone, very low hills
3	0.484	124	*Horizon*	29 July 53	Off Deep Plain, rolling plain
4	0.535	112	*Baird*	23 Nov 53	East of Hawaiian Arch, large rolling hills
5	0.561	107	*Baird*	3 Nov 53	West of Patton Escarpment, blocky steep hills
6	0.571	105	*Horizon*	3 Oct 53	South of Murray Fracture Zone, broad high hills
7	0.600	100	*Horizon*	4 Oct 53	South of Murray Fracture Zone, gently rolling deep sea fan
8	0.619	97	*Horizon*	4 Oct 53	Moonless Mountains
9	0.561	107	*Horizon*	26 Oct 53	Hawaiian Arch
10	0.577	104	*Horizon*	26 Oct 53	Hawaiian Arch, just east of #9
11	0.588	102	*Horizon*	26 Oct 53	Hawaiian Arch, just east of #10 subdued low hills with seamounts
12	0.571	105	*Horizon*	26 Oct 53	Hawaiian Arch, just east of #11, subdued low hills with seamounts

Table 1. Profile Data, North Pacific — Continued

Profile	Length of 3-min Interval (n mile)	No. of Intervals	Ship	Date	Character
13	0.571	105	*Horizon*	29 Sept 52	Murray Fracture Zone, top of main ridge, increasingly hilly to right
14	0.582	103	*Horizon*	30 Sept 52	Murray Fracture Zone, bottom of main ridge
15	0.632	95	*EPCER 857*	29 Sept 52	Abyssal plain with one deep sea channel
Average	0.571	105			

[1] from Krause and Menard, 1965.

1.4 Other Studies

Although the literature of quantitative geomorphology is extensive, very little of it applies to marine geomorphology. Many papers have dealt with various statistical aspects of bathymetry, such as Agapova (1965), McDonald and Katz (1969), Heezen and Holcombe (1965), Holcombe and Heezen (1970), Smith et al. (1965), and Switzer et al. (1964). Few, however, have dealt with the specific goals of this paper. More pertinently, McDonald et al. (1966) made a quantitative geomorphic examination of the USN *Thresher* search area in the northwestern Atlantic using our methods. Even though the area was much smaller and the slope distance interval was an order of magnitude shorter than this study, the slope distributions obeyed the same laws as presented here. Using deep-towed sonar in the eastern Pacific, Loughridge and Spiess (1968) also have shown fine-scale slopes (on the order of 100 m long) to have frequency distributions similar to those described in this paper. Spiess et al. (1969) and Larson and Spiess (1970) have further examined cumulative relations for fine-scale slopes but used a method different from that of this paper. A replot of their results gives very similar results to ours with linear log-log cumulative plots for slopes below 8 to 12 degrees (140 to 220 m/km), which represent 90 percent of the slopes encountered in their areas. They show that most of these slopes have linear extents of 100 m or less.

Table 2. Profile Data, South Pacific

Profile	Start Lat. (°S)	Start Long. (°W)	End Lat. (°S)	End Long. (°W)	Length (km)	Total Units	Shoalest depth (m)	Deepest depth (m)
1	34.99	119.48	35.00	118.26	110.6	104	802	3633
2	34.99	116.49	34.98	115.28	110.8	99	3424	3803
3	34.98	114.81	34.98	113.59	111.5	106	2340	3718
4	34.98	112.67	35.00	111.44	111.8	112	2397	3566
5	34.94	110.42	34.81	109.22	110.8	97	2990	3527
6	34.63	108.07	34.48	106.87	111.6	91	2907	3424
7	34.46	106.72	34.32	105.52	111.5	92	2924	3547
8	34.32	105.50	34.18	104.30	111.5	94	3064	3718
9*	34.46	106.71	34.18	104.31	221.8	184	2924	3718
10	34.18	104.31	33.95	103.12	110.7	95	3122	3758
11	33.95	103.10	33.77	101.92	111.0	92	2868	3796
12*	34.18	104.29	33.77	101.92	223.0	187	2868	3796
13	33.51	99.98	33.30	98.80	111.4	91	2943	3955
14	33.30	98.79	33.14	97.61	110.9	91	2661	3965
15*	33.50	99.96	33.14	97.61	222.3	181	2661	3965
16	32.99	96.53	32.88	95.35	110.8	92	3583	4102
17	32.79	94.60	32.66	93.42	111.2	97	2429	3968
18	32.51	91.95	32.40	90.77	110.8	115	2943	3908
19	32.39	90.72	32.30	89.53	111.7	95	2921	3813
20*	32.51	91.92	32.30	89.57	222.3	207	2921	3908
21	32.30	89.52	32.28	88.33	111.6	110	2745	3947
22	32.28	88.32	32.32	87.14	111.3	103	2924	4060
23*	32.30	89.52	32.32	87.15	222.9	212	2745	4060
24	32.37	86.23	32.45	85.04	111.6	91	3756	4095
25	32.45	84.99	32.54	83.80	111.5	95	3532	3984
26	32.37	86.23	32.54	83.87	221.9	187	3532	4095

Interestingly, at the Seattle meeting of the American Geophysical Union in 1964, E. Shoemaker presented radar results that suggest that slopes on the moon obey similar laws as presented here. Tyler et al. (1971) and Tyler and Simpson (1970) find root-mean-square (rms) lunar slopes about half as large as those found in this study at a length scale of 1 km and probably at smaller scales as well.

2. CONCEPTUAL MODEL

A complete understanding of the sea floor requires knowledge of the complete geological system, not only of the processes but also of the sources and the products. This study concerns a product, bottom slope, from which the generative processes might be inferred. Unfortunately, observational techniques do not allow complete knowledge of the slopes; therefore, statistical methods must be used. Similarly bottom slopes are randomized products of several geological processes. However, a conceptual model can be developed to describe the distribution of all slopes from statistical compilations of measurable slopes. The integrations of the model equations are directly analogous to the statistical summations performed during data collection and analysis as actually used in this study.

Assume that the frequency distribution of bottom slopes is an inverse exponential function of their actual slope and has the distribution of a hyperbola

$$s^n f = a \tag{1}$$

where s is the slope in meters/kilometers, f is the relative frequency of slope s, a is a constant, and n is a factor varying from zero to one (as will be shown later). The frequencies of all slopes cannot be measured in practice; therefore, slope frequenices are collected into frequency classes F of width Δ (5 m/km in this paper) and of midpoint slope s,

$$F = \int_{s-\frac{1}{2}\Delta}^{s+\frac{1}{2}\Delta} f \, ds = \int_{s-\frac{1}{2}\Delta}^{s+\frac{1}{2}\Delta} a s^{-n} \, ds$$

$$= \frac{a}{1-n} \left[(s+\tfrac{1}{2}\Delta)^{1-n} - (s-\tfrac{1}{2}\Delta)^{1-n} \right] \tag{2}$$

The summed frequency classes x are

$$x = \int_0^{s+\frac{1}{2}\Delta} as^{-n}ds = \frac{a}{1-n}(s+\tfrac{1}{2}\Delta)^{1-n} \tag{3}$$

$$x \cong \frac{a}{1-n} s^{1-n} \tag{4}$$

The cumulative slope compilation is derived as follows where y is cumulative slope

$$y = \int_0^s sfds = \int_0^s as^{1-n} ds$$

$$= \frac{a}{2-n} s^{2-n} . \tag{5}$$

Substituting x for s from (4)

$$y = \frac{a}{2-n} \left(\frac{1-n}{a}\right)^{\frac{2-n}{1-n}} x^{\frac{2-n}{1-n}} . \tag{6}$$

This has the form

$$y = kx^m \tag{7}$$

where

$$k = \frac{a}{2-n} \left(\frac{1-n}{a}\right)^{\frac{2-n}{1-n}} \tag{8}$$

$$m = \frac{2-n}{1-n} , \tag{9}$$

and conversely

$$n = \frac{m-2}{m-1} \tag{10}$$

$$a = \frac{1}{m-1} \, (km)^{\frac{1}{1-m}} \quad . \tag{11}$$

This then requires for relative frequency

$$k = \frac{1}{m} \, a(m-1)^{1-m} \quad , \tag{12}$$

and for percent frequency

$$k = a(m-1)^{1-m}/(m \cdot 100^m) \quad . \tag{13}$$

Thus k is not an independent parameter relative to m.

3. GEOLOGIC ENVIRONMENT

3.1 East Pacific Rise

The earth's crust is made up of several large plates that are moving relative to one another. New sea floor is formed where the plates move apart at the central oceanic rifts. Sea floor is destroyed in the trenches where the plates come together and sink into the earth's upper mantle (subduction zone).

Since our original paper, considerable research by numerous workers shows the main processes yielding abyssal hills have been a combination of volcanism and normal faulting at the median rifts of the ocean basins (e.g., Vogt et al., 1969); the details are still poorly understood. Later sedimentation over millions of years smooths and modifies that original topography. Modification can also occur through later volcanism and faulting; although such processes may be minor or localized, their regional extent is still unknown. (Because some readers will be from other scientific fields, a brief review of the geologic mechanism involved follows at the end of this section.)

The investigated sea floor in both the North and South Pacific is the surface of the same general feature, the East Pacific Rise. The North Pacific sea floor was formed on a portion of the East Pacific Rise, which has since ceased to be active as a spreading sea-floor rift (Atwater, 1970). The examined North Pacific sea floor ranges in age from 30 m.y. (million years) in the eastern profiles near North America to 80 m.y. (Atwater and Menard, 1970) in the western profiles near Hawaii. The South

ently forming. The studied South Pacific sea floor ranges in age from zero m.y. to 30 m.y. (Keller and Peter, 1968; Morgan et al., 1969; Herron

and Hayes, 1969; Herron, 1971, 1972) as discussed later. The studied North Pacific sea floor has been subjected to a higher sedimentation rate (Goldberg and Koide, 1962) for a longer time than the studied South Pacific sea floor, so that the North Pacific has a thicker blanket of sediment (Ewing and Ewing, 1967) and hence a more subdued topography. The initial spreading rates are similar, 5 to 8 cm/year (Le Pichon, 1968; Atwater, 1970; Herron, 1972). Because two-thirds of the Pacific was formed at the East Pacific Rise or at associated rises, this study is considered to be significant for sea-floor topography and its formation.

The floor of the southeastern Pacific Ocean consists of three tectonic plates: the Pacific to the west, the Antarctic to the south, and the Nazca to the northeast (Morgan et al., 1969; Herron and Hayes, 1969; Herron, 1971, 1972). These three plates meet in a triple junction of a rift-rift-transform fault type near 35°S 111°W. To the north, the Pacific and Nazca Plates are being generated along the rapidly spreading rift of the East Pacific Rise. To the southwest, the Pacific and Antarctic Plates are being generated along the rift of the Pacific-Antarctic Ridge. To the east, the Nazca and Antarctic Plates interact along the Chile Rise with a series of short spreading ridges offset by long dextral transform faults.

The Nazca Plate is being subduced (i.e., is sinking) beneath South America to its east. The Pacific Plate is being subduced far to the west along the western margin of the Pacific basin. The Antarctic plate is growing on all sides.

The sea-floor topography reflects the plate tectonic processes. Sharp, probably asymmetrical abyssal hills exist (Krause and Kanaev, 1970), which we know from studies elsewhere are parallel to the rift at which they form (Atwater and Mudie, 1968). These hills are cut transversely by fracture zones that are generated at the numerous transform faults that offset the given rifts. The low sedimentation rates combined with the rapid spreading rates mean that sediment is thin (less than 150 m, Hayes et al., 1972) out to considerable distances from the rift (i.e., 2000 km).

The topography is also a function of the width of the intrusion zone. Northrup (1972) has concluded that at present several zones along the Pacific-Antarctic Ridge and the East Pacific Rise are spreading with little release of strain energy as shown by low seismicity. He concludes that this implies a very narrow zone of intrusion; a conclusion born out by very sharp magnetic anomalies for late Cenozoic time (Hayes et al., 1969).

The topography is (Krause and Menard, 1965; see figs. 2 and 3): "...affected by the materials of the sea floor and the geologic processes which have modified the sea floor. The composition of the sea floor in this study can be broadly divided into three main components: (1) recent, soft sediments, (2) older, stiffer or consolidated sediments, and (3) lava flows. The processes locally modifying the sea floor can be broadly

divided into the following main groups: (a) pelagic sedimentation, (b) turbidity current deposition, (c) slumping of sediments, (d) tectonic deformation, and (e) volcanism. In certain cases, we can pinpoint the conditions. [North Pacific] profile 15, for example, was chosen to be typical of turbidity current deposition of recent, soft sediment. The steep slopes, especially the longer ones, are generally associated with volcanoes as in [North Pacific] profiles 8, 10, 11, and 12." The studied areas of the East Pacific Rise do not seem to be affected by deep bottom currents.

3.2 Geologic Interpretation of *Oceanographer* Profile

The *Oceanographer* profile crosses the East Pacific Rise along 35°S in the west to 32°S in the east. The area of specific concern in this paper lies between 120°-84°W. Depths range generally between 2500 to 3000 m at the ridge crest and between 3700 to 3900 m at the eastern end (84°W). From west to east, the sea floor has an age near 20 m.y. at 120°W, and gradually becomes younger until newly formed at 111°W. From thence it gets older (though not continuously) reaching 25 to 30 m.y. at 84°W. These interpretations are based on magnetic data of this and past studies (Keller and Peter, 1968; Morgan et al., 1969; Herron and Hayes, 1969; Herron, 1971, 1972).

The study area of the east-west *Oceanographer* profiles represents 3300 km across the East Pacific Rise. The trend of the abyssal hills here is inferred to be northerly so that the profile is approximately perpendicular to this trend. The profile crosses several fracture zones (at least seven) very obliquely. In most cases, they are readily identifiable by excessive depths, abrupt regional changes in depth, very rough topography, breaks in magnetic pattern, etc.

Several significant features appear:
1. At the western end, a group of seamounts exist. No others are present in the rest of this profile.
2. Two very prominent fracture zones are at the crest of the East Pacific Rise (111°W and 108.5°W).
3. An anomalous area of relatively elevated sea floor was crossed between 95 to 85°W.
4. Significant rounding of topography of sedimentation occurs only east of 87°W.

3.3 Ridge Crest

The *Oceanographer* profile crosses the ridge crest at 35°N, 111°W, very close to the "Chile triple junction" where the Pacific, Nazca, and Antarctic Plates join. A major fracture zone also crosses the ridge crest here, so that most of the central magnetic anomaly, and hence the active rift, are not present in the profile (Keller and Peter, 1968). USNS *Eltanin* cruise number ELT 24 (Hayes et al., 1969) crosses the ridge crest

slightly to the south. The central magnetic anomaly is very well developed there (111°W), as well as most anomalies out to 10 m.y. (anomaly 5 of the scale of Heirtzler et al., 1968). This *Eltanin* crossing shows a spreading rate of 4.8 cm/yr for the last 5 m.y. between the Pacific and Antarctic Plates.

The *Oceanographer* profile crosses a second major fracture zone at 108.5°W. These zones trend east-by-south, and this is the more northerly of the two. Along the profile, a spreading rate of 5.4 cm/year is calculated from the magnetic anomalies (less than 10 m.y. old) east of the ridge crest (east of 108°W). This 5.4 cm/year represents the rate north of the triple junction between the Pacific and Nazca Plates. This agrees with Herron's (1972) rate of 5 cm/year between 5 to 10 m.y. ago. She obtains 8 to 9 cm/year between 0-5 m.y. ago, a period that is in part absent on the *Oceanographer* profile. She obtains a transform rate of 6 cm/year across the Chile Fault between Antarctic and Nazca Plates. Note that the rift rates are the usual rift half rates; rates across analogous transform faults are twice these.

By inference therefore, one or both of the fracture zones represent the active Chile transform fault (that is, both if the zone of faulting is rather wide or if the faults are offset by a small spreading center). The earthquake epicenters can best be aligned with the northerly fracture zone (Barazangi and Dorman, 1968; ESSA, 1970), and so it is preferred as the active fault between the Nazca and Antarctic Plates.

The magnetic pattern of the zone between the two fracture zones can be interpreted as lying east of a rift, and hence the zone is herein assumed for discussion to be part of the Antarctic Plate. The profile west of 111°W is therefore over the Pacific Plate and the profile east of 108.5°W over the Nazca Plate.

3.4   Elevated Sea Floor

The elevated sea floor between 96 and 85°W was recognized as anomalous by Keller and Peter (1968) and considered by them to be the Chile Rise. They point out that the *Oceanographer* magnetic profile is not easily interpreted in the area. The studies by Herron and Hayes (1969), Morgan et al. (1969), and Herron (1971) show the active Chile Ridge to be to the south, but they do not solve the above problem of the elevated sea floor, failing to detect a magnetic pattern in the immediate area. They do point out that the pattern to the east of that region cannot be explained in terms of spreading along the present Chile Rise. We have attempted further interpretation of the complex *Oceanographer* profile and conclude that the elevated region is the residual ridge of an old rift. Quite independently (as often happens in an active science), Herron (1972) has concluded that such an ancient ridge exists to the north. Her evidence is massive and well presented. Her southernmost evidence shows the ancient ridge near 33°S, 94°W, somewhat west of our position. This suggests either (1) a fracture zone separates the two

positions, or (2) the ridge's trend is more westerly than shown. Alternate explanations of the elevated area can be rejected because of the fortuitous, but real, test provided by Herron's (1972) recognition of the ridge.

Herron (1972) concludes that the minimum age of this ancient rift is 10 m.y. and that it spread at 5 cm/year for the previous 10 m.y. On the basis of the identification of *Oceanographer* magnetic anomalies, we would put the minimum age rather older, though with the same rate over a 10 m.y. period. However, our evidence is inconclusive because of the disturbed nature of this region.

Our interpretation would put the ancient rift near 32.4°S, 90.7°W. At least two fracture zones are detected in the region. A moderate topographic symmetry axis exists about the 90.7°W position. A moderate magnetic symmetry axis also exists but incompatibly, slightly to the west (91.1°W) of the topographic symmetry axis. Certain tests are made in this paper for geomorphic effects: profile 18 lies immediately west of 90.7°W (90.77°W to 91.95°W), profile 19 lies immediately east (90.72°W to 89.53°W), and profile 20 includes both 18 and 19.

3.5 Bottom Topography as Formed Through Sea-Floor Spreading

Vine (1966) firmly established that new sea floor and oceanic crust are being formed at active sea-floor rifts. These exist at the boundary of two crustal plates that are slowly moving apart at rates of several centimeters per year. Magma oozes up the rift zone and eventually cools to a rock at which time it becomes welded to the adjacent crustal plate. Because the crustal plate moves everywhere at the same (angular) velocity, the sea floor at a given angular distance from the rift has the same age — the age at cooling (Le Pichon, 1968).

The lava that reaches the uppermost crust becomes magnetized in the earth's magnetic field as it cools through about 575°C. The direction of rock magnetism depends on the direction of the earth's field, which reverses about once or twice per million years (Vine, 1966). This reversal affects all crustal rock at the same time but only the cooling magma in a significant way. A magnetic pattern is imprinted on the cooled rock and is revealed by anomalies in the earth's magnetic field which are parallel to the rift. Because the rate of reversal is not constant, these anomalies have a pattern of spacing that depends on age — thus the age of cooling of the sea-floor rock at the rift can be determined from the magnetic anomaly's pattern.

The detailed sea-floor topography is formed at the rift by a combination of volcanism, collapse, and faulting; the details vary from place to place. But, beyond that simple statement the processes are generally poorly understood. The process is envisaged to proceed somewhat as follows:

1. The two crustal plates are slowly spreading apart at several centimeters per year.

2. Tholeiitic lava rises upward along the rift zone from depths of 50 to 100 km. Tholeiite is a type of basaltic magma characteristic of ocean basins (Engel and Engel, 1964).

3. At intervals measured in decades or centuries for a given location, the lava erupts in the rift zone. Conceptually, the lava should approximately fill the rift zone. However, the general case may be one of either overfill or underfill. In due course, the eruption ceases (measured perhaps in months). The lava and its subterranean equivalents begin to cool.

4. The plates continue to spread (though not necessarily smoothly). Because lava cannot rise through cracks less than a few meters wide (McConnell, 1967; Szekely and Reitan, 1971), considerable cracking of the cooling lava and its surrounding older rock occurs, eventually accompanied by collapse of rock into slowly opening fissures. Steep scarps form facing the rift. The process is very much like caldera formation in active volcanoes when a subterranean magma reservoir is emptied. Very large blocks may slump in toward the rift if eruptions do not occur for several centuries or millenia. By inference, the side of an abyssal hill facing rift will be highly faulted while the side facing away will be largely constructional, having been formed during the lava eruptions.

The basic form of the ridge has been attributed by McKenzie and Schlater (1969) to cooling of the lithosphere and mantle away from the rift. Sclater and Francheteau (1970) and Sclater et al. (1971) give theoretical equations giving the form of a ridge if the spreading rate is known (or vice versa). Fracture zones are formed along the active transform faults that offset individual segments of a rift zone. At either end, these faults are often deeper than the rift zone. Such fracture zones have been considered to be generally inactive once the topography is carried by the plate beyond the active rift. However, minor vertical adjustments must take place because the plate on either side of the fracture cools and hence sinks at different rates — rates that are a function of distance from the rift.

4. METHODS

4.1 General

A conventional echo-sounding profile is an imperfect representation of the sea floor, because the most commonly used echo sounder transducer emits and accepts sound pulses through a vertical solid angle of 30° between half-power points (Krause, 1962). The sounder does not record the true shape and slope of hilly bottom, because point reflectors on the hills give hyperbolic echo traces (Hoffman, 1957; Krause, 1962). The conventional echo sounder records the vertical depth only where the sea floor is horizontal and the sea is calm. Thus, the depth recorded is rarely from beneath the ship, and the recording inherently smooths the irregularities of the floor. Only generalized information can be obtained from such echo-sounding profiles. In contrast, the narrow-beam sounder of 3° width gives much more information about the sea floor because the depth recorded is in the true vertical (Krause and Kanaev, 1970). Thus, care must be taken not to proceed beyond the limits of the assumptions and errors involving specific instruments, including navigational errors.

In the North Pacific, the depths are measured at about 1-km (0.57 n miles) intervals. The derived slopes are integrated so that irregularities less than 1 km wide are removed, as well as any effect of the hyperbolic echo trace from a single point of the sea floor. Had depths been read at half the above distances, the slopes would have been those of the hyperbolic echo rather than those of the sea floor. For slopes up to 15° (130 fm/0.5 n miles; 260 m/km), the difference between the true and recorded slopes is small for a track perpendicular to the slope and, therefore, is disregarded in this paper. Steeper local slopes have little effect on the integrated slope.

In the South Pacific study, the depths were measured at about 1.26 km intervals, but significant intermediate inflection points were measured as well. Thus the derived slopes are integrated slopes of 0.20 to 1.31 km long. Because a narrow-beam echo sounder was used, no effect of a hyperbolic echo trace is present. Potentially a great deal more detailed information on slopes is available on the South Pacific echograms than on the North Pacific ones.

In both studies, the profiles were oriented perpendicular to the regional topography (where significant). In the South Pacific study, the profiles were carefully selected to avoid including the crossings of fracture zones. The topography in both studies is inferred to be composed of elongate ridges, many times longer than wide, parallel to the rift zones. These ridges when less than 1000 m high are classified as "abyssal hills." Different ships' courses that cross these ridges of course yield different slope distributions. A course perpendicular to the regional trend will yield the profile with the steepest slopes and the most topographic features crossed. This will vary with a ship's course until one parallel to the regional trend will yield the most subdued profile. The perpendicular profile was chosen to give the most reproducible results and is expected

to yield the best relationships. The derived distributions and parameters are felt to be unique for such a profile and can be used for classification.

The original South Pacific data were handled as follows. Depths were read and verified to the nearest fathom at each 2.5 min interval and at significant intervening peaks and troughs. Navigational data were collated; they consisted of satellite navigation fixes, speed changes, and course changes with times. These data were then punched on cards and computer processed, producing depths in fathoms and meters corrected for sound velocity with Matthews' (1939) tables. Each depth is accompanied by its position in latitude and longitude and in nautical miles of kilometers along the profile. The original South Pacific data are available from the NOAA Environmental Data Services upon request.

4.2 Improvements

The technique used in dealing with the South Pacific data is improved over the North Pacific data as follows:

1. Vertically stabilized narrow-beam echo sounder with precision recorder versus conventional Edo echo sounder.

2. More accurate satellite navigation with frequent fixes versus celestial navigation.

3. Depths are corrected for sound velocity.

4. Depths of significant peaks and troughs of the topography are used in addition to the depths at the standard distance interval.

5. As near as possible, the ends of the profile were selected to give the same depth.

6. Computer processing that allowed more profiles to be processed and each much more completely.

4.3 Frequency Distribution of Depths

To find the frequency distribution of depths, the profiles are divided into depth intervals. The frequency of a given depth is found as a frequency percent of the total length of profile occurring at that depth. For the South Pacific depth distribution analysis, the 26 profiles were divded into depth classes of 25 m each. For presentation of depth frequency distribution, these classes have been enlarged to 50 m thereby reducing much of the random irregularity of the 25-m classes (fig. 7). For the North Pacific, the depth interval is 20 fm (36.6 m) except for the very steep profile, 8, where a 50-fm (91.5 m) interval is used. All profiles are approximately 111 km long (60 n miles) except for certain of the South Pacific ones which are twice as long (9*, 12*, 15*, 20*, 23*, and 26*) and marked with an asterisk.
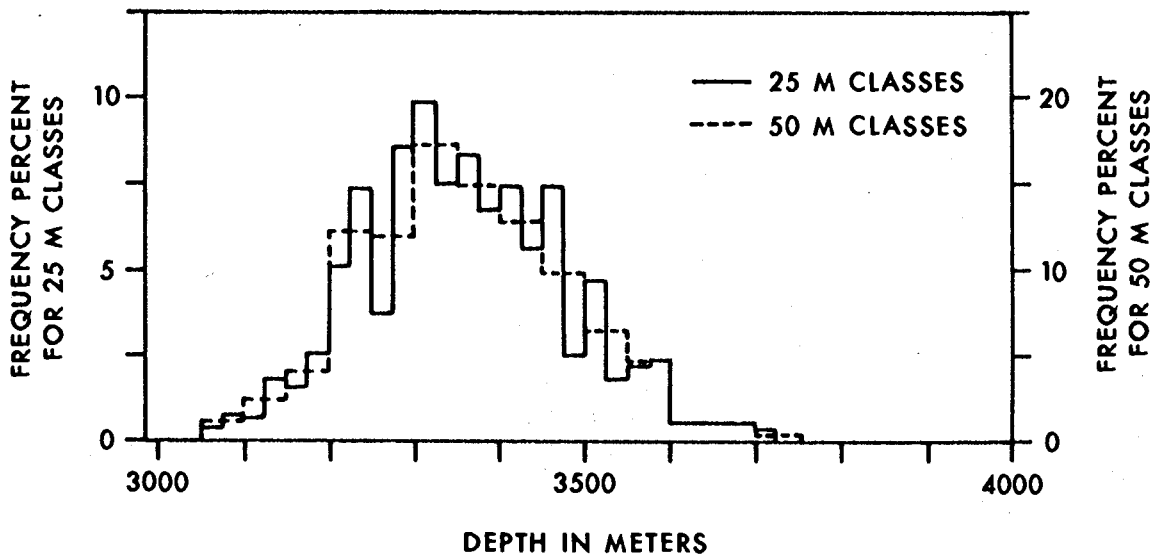
Figure 7. Comparison of depth frequency distribution for 25-m and 50-m class intervals using South Pacific profile 8 as an example.

Various statistical measures (listed below) have been calculated for depth intervals of 25 m and on a logarithmic scale from 1 to 10 with intervals at relative units of 0.5. Parameters based on a 50-m interval are insignificantly different from those of the 25-m interval and are not reported here. The logarithmic scale is used to test for log-normal distribution. The depth range of a profile is adjusted so that the shoalest depth = 1 and the deepest depth = 10.

Statistical parameters calculated are the following (Smith, 1966; Krumbein and Graybill, 1965):

mean

variance (not reported): $\Sigma(x-\text{mean})^2 \cdot \text{freq}(x)$

skewness (not reported): $\Sigma(x-\text{mean})^3 \cdot \text{freq}(x)$

kurtosis (not reported): $\Sigma(x-\text{mean})^4 \cdot \text{freq}(x)$

deviation: $(\text{variance})^{\frac{1}{2}}$

coefficient of skewness: $(\text{skewness})^{1/3}$

coefficient of relative skewness: $(\text{skewness})^{1/3}/\text{deviation}$

coefficient of kurtosis: $\text{kurtosis}/(\text{variance})^2$

chi square and degrees of freedom

median depth and depth percentiles of 2.28, 15.87, 84.13, and 97.72 percent

shoalest depth and deepest depth.

These statistical parameters have two functions: (1) to characterize the profile, and (2) to test Krause and Menard's (1965) conclusion that depths are normally distributed.

4.4 Frequency Distribution of Slopes

Slopes of the sea floor are calculated by finding the difference in depth per unit distance. In the South Pacific, slopes are measured between depth points in units of 1.83 m (1 fm), changed to units of meters per kilometer, and then collected into classes with units of 5 m/km. In the North Pacific, slopes were measured to the nearest 5 fm (9 m) over unit distances that represent 3 min of running time; this varies from 0.484 to 0.632 n miles (0.897 to 1.171 km) depending on the profile (table 3). For plotting and tabulating slopes, a time interval was a more practical unit than distance; for most slopes, the error is negligible. Where important in the North Pacific analyses, the time results are corrected for distance.

Table 3. *Slope in Meters per Kilometer, Fathoms per 0.571 Nautical Mile, and Degrees*

m/km	fm/0.571 n miles	deg.	m/km	fm/0.571 n miles	deg.
5	2.9	0.3	100	57.8	5.7
10	5.8	0.6	125	72.3	7.1
5	8.7	0.9	150	86.7	8.5
20	11.6	1.1	175	101	9.9
25	14.5	1.4	200	116	11.3
30	17.3	1.7	250	145	14.0
35	20.2	2.0	300	175	16.7
40	23.1	2.3	350	202	19.3
45	26.0	2.6	400	231	22.8
50	28.9	2.9	500	289	25.6
55	31.8	3.2	600	347	31.0
60	34.7	3.4	700	405	35.00
65	37.6	3.7	800	462	38.6
70	40.5	4.0	900	520	42.0
75	43.4	4.3	1000	578	45.0

For comparison, slopes were compiled in three ways: uphill along the ship's course, downhill, and the two combined. As will be shown, a difference is to be expected because the origin of the abyssal hills tends to impose an asymmetrical shape upon them.

4.5 Cumulative Distribution of Slopes

The plot of cumulative slope distribution is not standard. Slopes are measured as depth difference per unit distance. In the South Pacific study, the distance unit is 1 km. In the North Pacific study, the unit is a distance interval covered by a ship in 3 min, averaging 0.571 n miles (1.05 km), and averaging 105 intervals per 60 n mile profile (varying from 95 to 124 intervals). In the South Pacific, the slope frequency is measured as percent of the profile (111 or 222 km long) covered by a given slope in 5-m units). In the North Pacific, the slope frequency is measured as the number of the intervals covered by a given slope (in 5-fm units). Note that fortunately this interval is not too dissimilar to percent. The frequency should be calculated as relative frequency as will be explained later.

The cumulative slope distribution is a plot of cumulative slopes vs. their cumulative frequency — in other words, a plot of cumulative elevation (y) vs. distance as measured in percent or intervals (x) beginning with zero slope:

$$y = 5b + 10c + 15d + \ldots + (s-5)\cdot u + sv \tag{14}$$

$$= \sum_{i=1}^{n} s_i \cdot f_i \tag{15}$$

and

$$x = a + b + c + d + \ldots + u + v \tag{16}$$

$$= \sum_{i=1}^{n} f_i \tag{17}$$

where $a, b, c, d, \ldots, v$ are the relative frequency (f_i) (or number of intervals) of sea-floor slopes (s_n) of 0, 5, 10, 15, . . ., s m/km (or fm/interval), respectively. The product of the frequency b of 5-m slopes times 5 m is plotted at a point (a + b, 5b); then the product of the frequency c of 10-m slopes times 10 m is added to the above product and the sum is plotted at point (a + b + c, 5b + 10c), etc.

Note that the cumulative slope distribution has no relationship to the height of the abyssal hills. The analytical effect of separating the uphill and downhill slopes is to transform the profile into a single large

seamount with sides of ever-changing slope from the steepest at the top to the gentlest (and flat) slope at the base. For the North Pacific study, the difference in total height between the cumulative uphill slopes and the cumulative downhill slopes is the difference in depth between the start of the profile and its end. As an improvement, the South Pacific profiles are chosen so that the two ends of any profile are approximately the same depth. The difference in cumulative frequency (or intervals) x between the two plots is a measure of the asymmetry of the hills.

As will be shown, the cumulative slope log-log plots tend to be straight lines or straight line segments. Such a straight line has the equation

$$y = k \, x^m \, ,$$
(7), (18)

or

$$\log_{10} y = m \cdot \log_{10} x + \log_{10} k$$
(19)

where y and x are defined earlier, and m and k are parameters.

For the North Pacific, m and k were calculated for curves or segments of curves chosen by inspection as being straight. To relate the parameters for the North Pacific study, the units of x were changed to standard distance units by multiplying x by a/a_0, where a is the distance traveled by the ship in 3 min for that particular profile and a_0 is a standard distance (0.571 n miles/3 min).

For the South Pacific, parameters m and $\log_{10} k$ were calculated for (1) the curve between each data point of non-zero relative frequency (i.e., between each plotted slope on the cumulative curve), and (2) the curve between every 10 such data points. For example, for case (2), if no zero frequencies occurred, the sets would correspond to the values of the curve corresponding to bottom slopes of 0.005 and 0.055, 0.010 and 0.060, 0.015 and 0.070, etc. If the frequency of slope 0.055 were zero, then the sets would be 0.005 and 0.060, 0.010 and 0.065, 0.015 and 0.075, etc. Such "decade" parameters essentially smoothed the curves. The number of decade parameter sets generated for each curve is (n-11), where n is the number of slope classes of non-zero frequency in a given profile.

Values are calculated for the east-facing slopes, the west-facing slopes, and for the combined slopes. The decade calculations are considered to be better average values, but the results are not significantly different from the first case.

The form of the calculations is as follows

$$m = \frac{\log_{10} y_2 - \log_{10} y_1}{\log_{10} x_2 - \log_{10} x_1} \tag{20}$$

and

$$\log_{10} k = \log_{10} y_1 - m \cdot \log_{10} x_1 \tag{21}$$

where x_1, y_1 and x_2, y_2 are successive values of x, y.

The results are *not* the same if percent frequency is used instead of relative frequency where

$$P = 100 \; x \; . \tag{22}$$

This is approximately the form of the North Pacific calculations. Although parameter m is unchanged from (20):

$$m = \frac{\log_{10} y_2 - \log_{10} y_1}{\log_{10} P_2 - \log_{10} 100 - \log_{10} P_1 + \log_{10} 100}$$

$$= \frac{\log_{10} y_2 - \log_{10} y_1}{\log_{10} P_2 - \log_{10} P_1} \tag{23}$$

parameter $\log_{10} k$ does change from (21):

$$\log_{10} k = \log_{10} y_1 - m \cdot \log_{10} P_1 + m \cdot \log_{10} 100$$

$$= \log_{10} y_1 - m \cdot \log_{10} P_1 + 2m \tag{24}$$

by a factor of $(+2m)$. Equation (19) becomes

$$\log_{10} y = m \cdot \log_{10} P + \log_{10} k - 2m . \tag{25}$$

If (14-19) are calculated with percent frequency rather than relative frequency, then the parameter k is different. Hence, relative frequency is favored over percent frequency.

The characteristic plot of the North Pacific m, $\log_{10} k$ was plotted in the above form because, rather coincidentally, the total number of slope intervals equalled approximately 100.

The maximum cumulative relative frequency for the combined slopes is 1.0. The maximum such frequency for east- or west-facing slopes will average near 0.5 plus a small additional frequency for zero slopes; the maximum varies between extremes of 0.424 to 0.633. As a test, the east- and west-facing slope frequencies were normalized to total 1.0 and calculations were performed, but the results are less regular and thus are not reported.

The South Pacific data are calculated both as relative frequency and as percent frequency. The former gives the simplest relations, while the latter compares with the North Pacific data.

The parameters m and $\log_{10} k$ vary. If one characteristic parameter set for a profile is to be chosen, some criteria must be used. As described later in section 5, suitable parameter sets can be handpicked to represent the most important part of the profile. For frequency as percent, this is the best method because $\log_{10} k$ varies over a wide range. However for relative frequency, $\log_{10} k$ varies very little; thus, machine selection is reasonable by finding a weighted mean and its standard deviation. The relative frequency must be weighted to get a characteristic parameter set (both m and $\log_{10} k$) because the high slopes contribute relatively little to the overall curve. For mean and standard deviation calculations between each data point of slope and relative frequency, the simplest suitable weighting factor is the square of the relative frequency associated with the parameter. For calculations between each 10 such data points, the simplest weighting factor is the cube of the relative frequency.

5. RESULTS

5.1 Frequency Distribution of Depths

North Pacific[1]. Profiles 1 through 5 and perhaps profile 15 have symmetrical, roughly unimodal depth distributions (fig. 8). Profiles 7, 8, 10 through 14 have depth distributions skewed so that the mode is deeper than the median, and in several, a long tail to the curve persists to shallower depths (fig. 8).

An inspection of the profiles (figs. 2 and 3) reveals an explanation
of these depth distributions. Profiles 1 through 5 show more or less uni-
form province of abyssal hills and exhibit symmetrical depth distributions
(fig. 8). Profiles 8 and 10 through 13 show seamounts and/or isolated
large abyssal hills that cause the pronounced skewness of the depth dis-
tribution. The large features add a segment of shallower depths to a
probable symmetrical depth distribution of a uniform province of abyssal
hills. Also note that in profile 8 (fig. 2), the two left profiles of
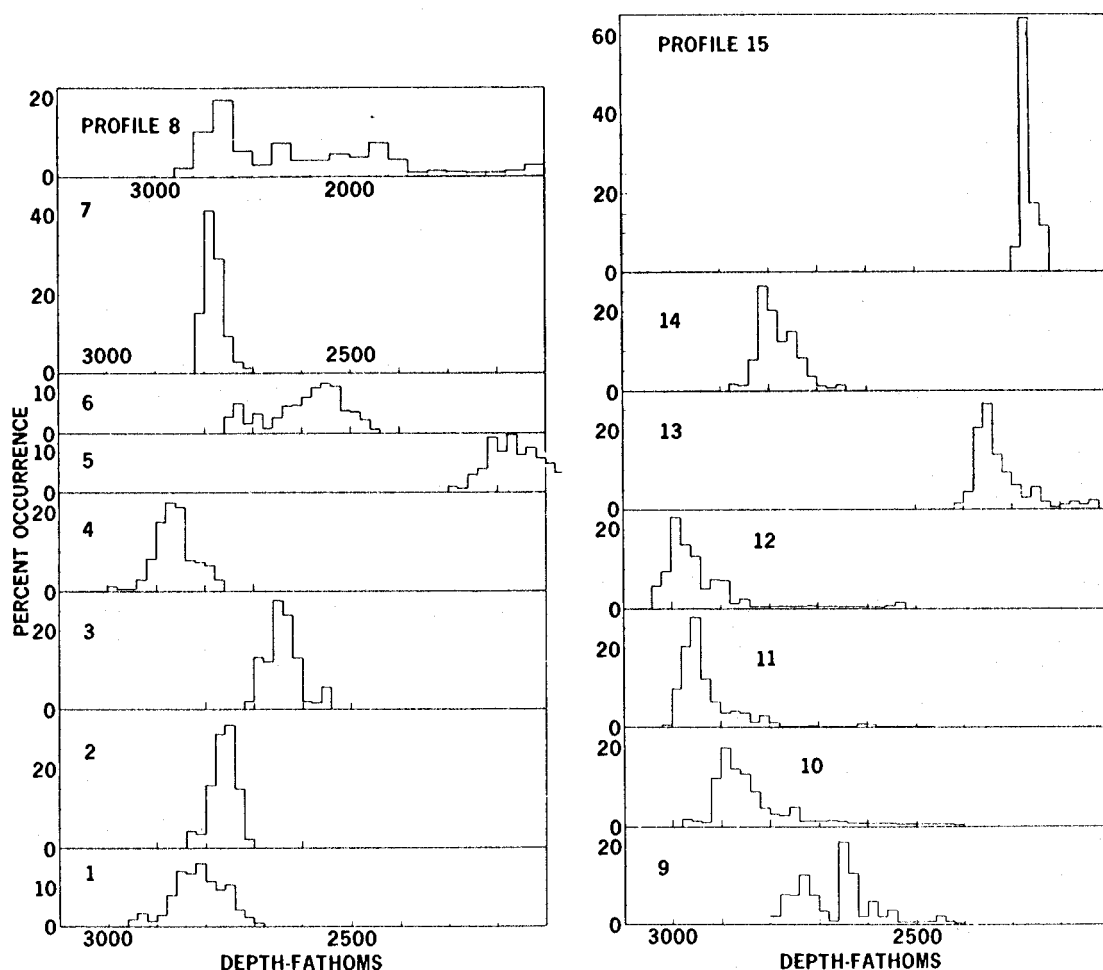
Figure 8. *Depth frequency distribution of North Pacific bathymetric pro-
files (from Krause and Menard, 1965).*

---

[1] Section taken almost unmodified from Krause and Menard (1965).

seamounts appear to be oblique crossing compared with the right profile, which appears to be directly over the seamount's crest.

The reason for the bimodal depth distribution (fig. 8) of profiles 6 and 9 is apparent in the inspection of the actual profiles where two distinct levels are seen. The skewed depth distribution of profile 7 must be due to isolated low abyssal hills that rise above a very subdued surface.

The symmetrical depth distributions of profiles 1 through 5 do not show a prominent level for the tops of the hills nor for the depressions between. The mode appears to coincide with the average depth of the region. We are apparently dealing with the random distribution of effects about a mean produced by specific causes. This suggests that a uniform process or series of processes led to the formation of the province of abyssal hills shown in a specific profile. Vertical tectonic faulting and volcanism would have a strong tendency to yield such a distribution, because the mechanical energy of formation of a vertical column on the sea floor is proportional to the square of its height from the mean sea floor depth assuming constancy of volume (Krause and Menard, 1965). The higher the hill, the more energy is required for its formation.

The cumulative distribution of depths in each profile was compared (fig. 9) with a normal distribution (a bell-shaped frequency distribution). Whether the distribution should be normal is a question that may be asked of nature. As a qualitative judgment based on the study of these few profiles, a uniform-appearing profile seems to have a normal distribution of depth, which may suggest a simple geological history. Profiles 1 through 5, 14, and 15 show normal or near-normal distributions, but others are skewed or polymodal. These seem to result from one geologic process, such as volcanism, superimposed over another, such as simple deformation, as in profiles 10 through 12 where the seamounts, which are obviously volcanoes, stand high above the abyssal hills. The volcanoes have a far different geologic history than the abyssal hills, and this may be seen from the depth distributions (figs. 8 and 9).

South Pacific. The results from the South Pacific (figs. 10, 11, 12, and 13) are in every way comparable with those from the North Pacific. The results support Krause and Mendard's (1965) conclusion that the depth distribution tends toward a normal distribution. The distributions were tested using the chi square test (table 4) (Smith, 1966; Krumbein and Graybill, 1965). Six profiles are normal at the 5 percent level (4, 7, 8, 9*, 10, and 17). Another profile (12*) is normal at the 10 percent level and the rest range upward from there. Two of the normal profiles are strongly multimodal (4, 10). Profiles 7, 8, and 9* are of irregular but moderate relief. In addition, five other profiles (2, 6, 24, 25, 26*), all of low relief, have a strong central tendcy but have moderate to high chi square percentiles. Such low relief profiles have only a limited depth range, so that a broad mode of a large secondary mode in any depth class strongly degrades the chi square value.
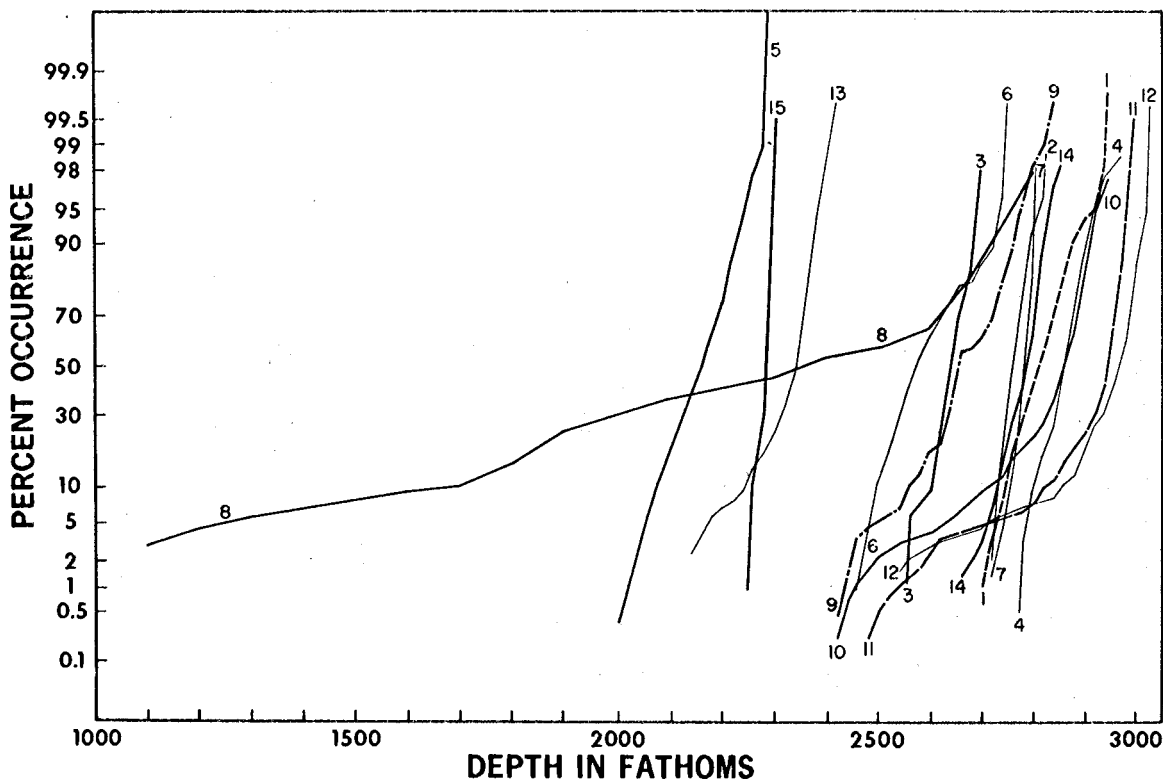
*Figure 9. North Pacific depth distributions as plotted on "probability"
graph paper (from Krause and Mendard, 1965).*

The skewed nature of many depth distributions led to a test for
log-normal distributions. Eight profiles are improved in chi square per-
centiles (6, 11, 12*, 13, 18, 19, 20*, 22) but only three are log-normal
at the 10 percent level (12*, 19, 10*), one of these (Profile 12*) is
also normal at the same 10 percent level (table 5). The skewness and/or
kurtosis improved for 15 profiles when the distributions transformed to
a logarithmic scale (table 4). Thus, depth distributions do tend toward
a normal distribution despite their skewed nature rather than to a random
or log-normal distribution.

The median depth generally is slightly deeper than the mean depth
(table 4). The mean or median depth corresponds to a modal depth in 19
of the 26 profiles (table 6, fig. 14). Ten profiles have two or more
prominent modes. In addition, five others have minor modes generally
representing the crests of peaks or the bottoms of troughs. In 12 out
of 16 cases, the mean or median depth coincides with the mode in uni-
modal profiles or in profiles with one major mode. Thus, the mean or
median depth usually corresponds to the mode in strongly unimodal depths
and usually corresponds to one of the modes in multimodal profiles
(table 7).

Figure 11. Depth frequency distribution of South Pacific profiles 10 to 15.

Figure 10. Depth frequency distribution of South Pacific profiles 1 to 9.
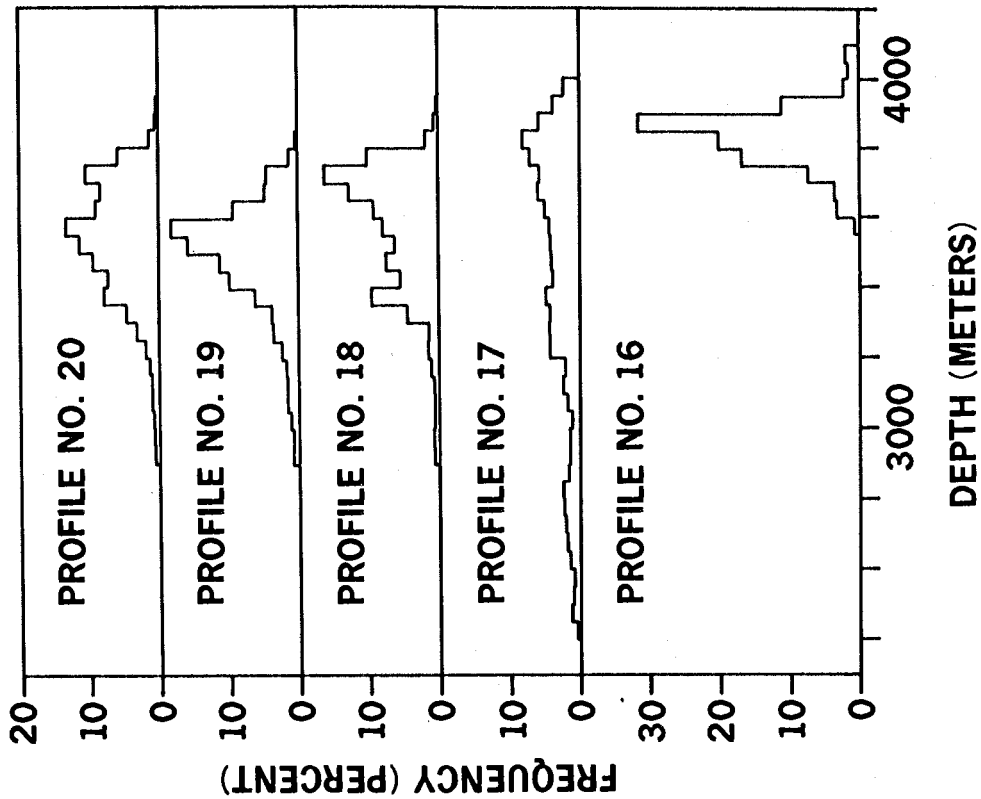
Figure 12. Depth frequency distribution of South Pacific profiles 16 to 20.
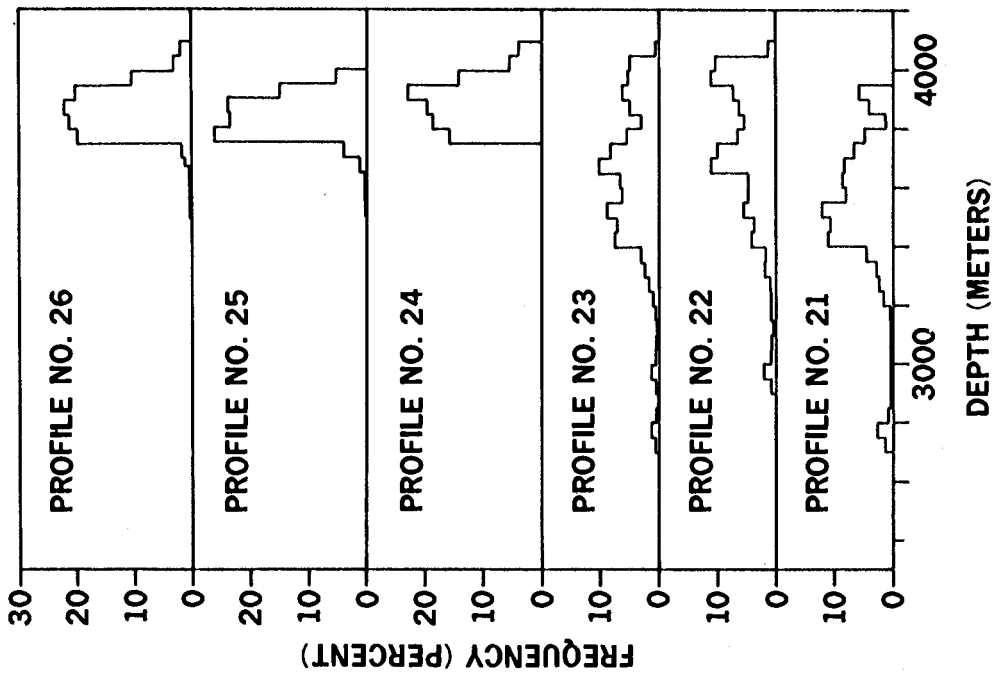
Figure 13. Depth frequency distribution of South Pacific profiles 21 to 26.

Table 4. *Statistical Parameters for Depth Distribution of Profiles Using 25 m Intervals. The lower the chi square percentile is, the better the distribution fits a "normal" error" or Gaussian distribution.*

Profile	Median Depth (m)	Mean Depth (m)	Deviation (m)	Coefficient of Skewness	Coefficient of Relative Skewness	Coefficient of Kurtosis	Degrees of Freedom	Chi Square	Percentile (less than)
1	2424	2470.9	820.1	-410	-.50	1.6	111	106	40
2	3634	3635.2	88.4	26	.30	2.1	14	21	90
3	3276	3186.2	300.9	-250	-.82	2.4	53	62	80
4	3047	3043.1	250.3	-170	-.66	2.5	45	26	1
5	3229	3220.4	130.3	48	.36	2.1	20	19	50
6	3244	3230.8	86.0	- 85	-.99	4.3	18	31	97.5
7	3235	3231.0	131.9	62	.47	2.7	23	12.3	5
8	3353	3359.4	119.4	74	.62	2.9	24	8.3	0.5
9*	3294	3294.8	141.7	39	.27	2.8	30	5.7	0.05
10	3468	3465.7	128.3	- 61	-.48	2.3	24	8.8	0.5
11	3580	3520.2	191.6	-210	-1.08	4.0	35	80	99.9+
12*	3533	3492.5	165.0	-150	-.93	3.6	36	24	10
13	3622	3624.8	195.0	-180	-.90	3.9	39	56	97.5

Table 4. Statistical Parameters for Depth Distribution of Profiles Using 25 m Intervals — Continued

Profile	Median Depth (m)	Mean Depth (m)	Deviation	Coefficient of Skewness	Coefficient of Relative Skewness	Coefficient of Kurtosis	Degrees of Freedom	Chi Square	Percentile (less than)
14	3575	3426.1	390.8	-320	-.82	1.9	50	80	99.5
15*	3607	3525.7	324.2	-330	-1.02	3.3	50	60	90
16	3846	3834.5	87.5	-48	-.55	3.9	19	22	70
17	3520	3433.0	389.8	-350	-.90	2.6	59	41	5
18	3606	3560.9	185.1	-180	-.97	3.6	37	55	97.5
19	3510	3481.5	166.1	-170	-1.00	4.1	34	43	90
20*	3540	3517.7	181.4	-170	-.92	3.6	38	33	30
21	3538	3532.5	251.1	-260	-1.04	5.1	46	117	99.9+
22	3731	3711.9	257.0	-260	-.99	3.8	44	96	99.9+
23*	3645	3621.0	268.8	-260	-.95	4.2	51	63	90
24	3883	3890.5	80.7	59	.73	2.5	11	11.5	60
25	3833	3838.2	68.3	-39	-.57	3.5	16	30	99
26*	3860	3867.9	78.6	50	.63	3.3	20	15.2	30

-31-

Profile	Coefficient of Relative Skewness (log)	(25m)	Coefficient of Kurtosis (log)	(25m)	Chi Square	Percentile (less than) (log)	(25m)
3	.55	-.82	(2.1)[1]	2.4	(35)	(99.9)	80
6	.68	-.99	3.6	4.3	13	40	97.5
11	-.61	-1.08	2.7	4.0	(34)	99.9	99.9+
12*	.60	-.93	2.7	3.6	8.1	*10*[2]	10
13	.73	-.90	2.4	3.9	18	80	97.5
14	.45	-.82	(1.8)	1.9	86	(99.9+)	99.5
15*	-.44	-.1.02	(2.2)	3.3	(33)	(99.5)	90
17	.40	-.90	(1.9)	2.6	(22)	(90)	5
18	-.37	-.97	2.1	3.6	20	90	97.5
19	.62	-1.00	3.0	4.1	8.6	*10*	90
20*	.61	-.92	2.5	3.6	6.5	*5*	30
21	.85	-1.04	3.2	5.1	(39)	(99.95)	99.9+
22	.45	-.99	2.0	3.8	25	95	99.9+
23*	.75	-.95	2.4	4.2	(25)	(95)	90
25	(.89)	-.57	2.8	3.5	(34)	(99.95)	99

[1] Inferior values bracketed.

[2] Log-normal distribution indicators of 10% or less are in italics.

Excluding profile 1 of seamounts, the deviation from the mean depth ranges from 68 to 391 m and of course highly correlates with the relief of the profile (table 4). Most of the profiles are skewed toward deeper depths (negatively skewed), which is the effect of small sea peaks giving shoaler depths than the general depth of abyssal hills in a given profile. The relative kurtosis coefficient is a measure of the distribution of the shallow and deep tails of the profile, a value of 3 being typical for a normal distribution.
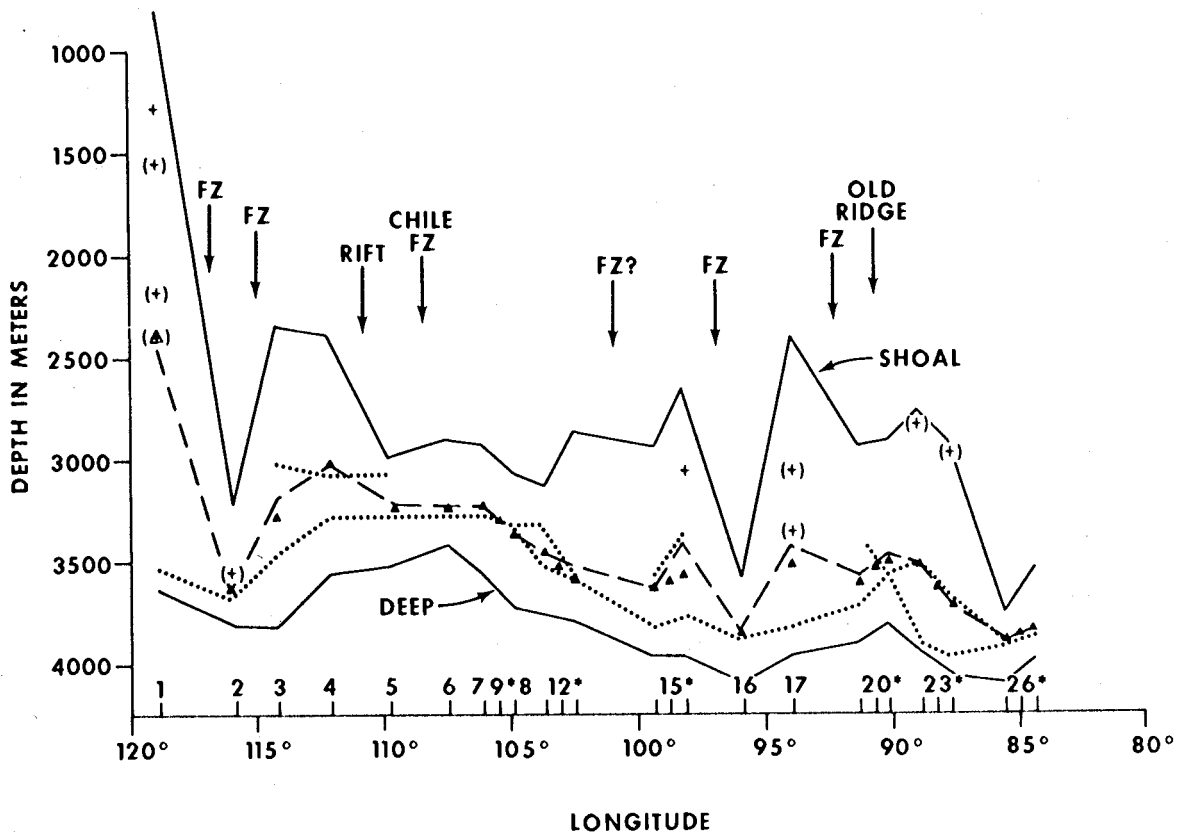
Figure 14. Depth parameters of the 26 South Pacific profiles plotted along their length. Plotted parameters are shoalest and deepest depths (solid lines), mean depth (dashed line), median depth (triangles), principal modes (dotted line and crosses, in parentheses where weak).

The comparison of the 12 selected 111-km profile pairs with their six 222-km equivalents yields expected results. In general, the shorter profiles show more sharply defined modes than do the combined profiles, which show smoother distributions. In all cases except profile 10 which even shows a strong normal tendency, the combined distributions are closer to normal distributions than the shorter profiles, expecially where the shorter profiles have normal distributions and are not very different in regional depth; e.g. profiles 7, 8, 9* and 24, 25, 26*. In two cases, the pair has quite differently skewed distributions, but the combined distribution is not extremely skewed (10, 11, 12* and 18, 19, 20*). In the latter profiles, the shoaler parts (2900 to 3400 m) of the distributions are quite similar to each other but the deeper parts dissimilar. Each profile of the remaining pairs (13, 14, 15* and 24, 25, 26*) is quite dissimilar; in one case (15*), the combined distribution is somewhat more regular though skewed; in the other case (23*), the combined distribution is more multimodal because of dissimilar modes in the individual profiles of the pair.

Table 6. Modes of Depth Distribution for 50-m Intervals.

Profile	Modes in Meters				
1	1275,	(1550)[1],	(2175),	(2425)[2],	3525
2			3575,	*3675*	
3	3025,		3475		
4	*3075,*	3275			
5	3075,	*3275*			
6		*3275*			
7		*3275*			
8		*3325*			
9*		*3275*			
10		3325,	3525		
11			*3575*		
12*			*3575*		
13			*3575,*		3825
14	2825,	(3375),		3775	
15*	(2825),			3775	
16					*3875*
17	(2825),	(3375),			3825
18		(3375),		3725	
19			3575		
20			*3575,*	(3725)	
21	(2775),		*3525,*		(3925)
22		(2975),		*3675,*	3975
23*	(2775),	(2975),	3525,	*3675,*	3925
24					*3925*
25					*3825*
26					*3875*

[1] Weak or dominated modes in parentheses.

[2] Modes in italics are within 50 m of the mean and/or median depth.

Table 7. Importance of "Mean" Depth as a Description of the Profile, South Pacific.

Highly Pertinent: strong central mode		Somewhat Pertinent	Unapplicable: bi- or multi-modal or very highly skewed frequency depth distribution
Profile		Profile	Profile
2	16	11	1
5	19	13	3
6	21	18	4
7	24	20*	14
8	25		15
9*	26*		17
10			22
12*			23*

The relief of the profiles (including those already mentioned) can be summarized as follows: low relief (2, 6, 24, 25, 26*); irregular but moderate relief (7, 8, 9*); relief containing sharply peaked hills but generally homogeneous (10, 11, 12*, 16, 18, 19, 20*); high but homogenous relief (1, 14, 17). Finally, the remaining eight profiles show multi-modal distributions (3, 4, 5, 13, 15*, 21, 22, 23*). Several of these modes can be related to specific aspects of the relief. For example, the shallowest modes of several profiles can be identified with an individual high hill on the profile. Profiles 3 and 4 show two main levels with the deeper on a gentle plain and the upper quite irregular. Most of the modes of the other distributions can be similarly correlated to relief.

Hence given homogeneous relief, the depth distribution tends to normal. If sharp peaks are added, the distribution becomes skewed. Finally if several uniform elements are combined in a single profile, a multi-modal distribution exists and each mode can be correlated to its element.

5.2 Frequency Distribution of Slopes

North Pacific. The frequency distributions of the slopes (fig. 15) show typically a small amount of flat bottom, a frequency peak at a slope near 5 to 10 fm per interval (about 9 to 17 m/km), a minimum near
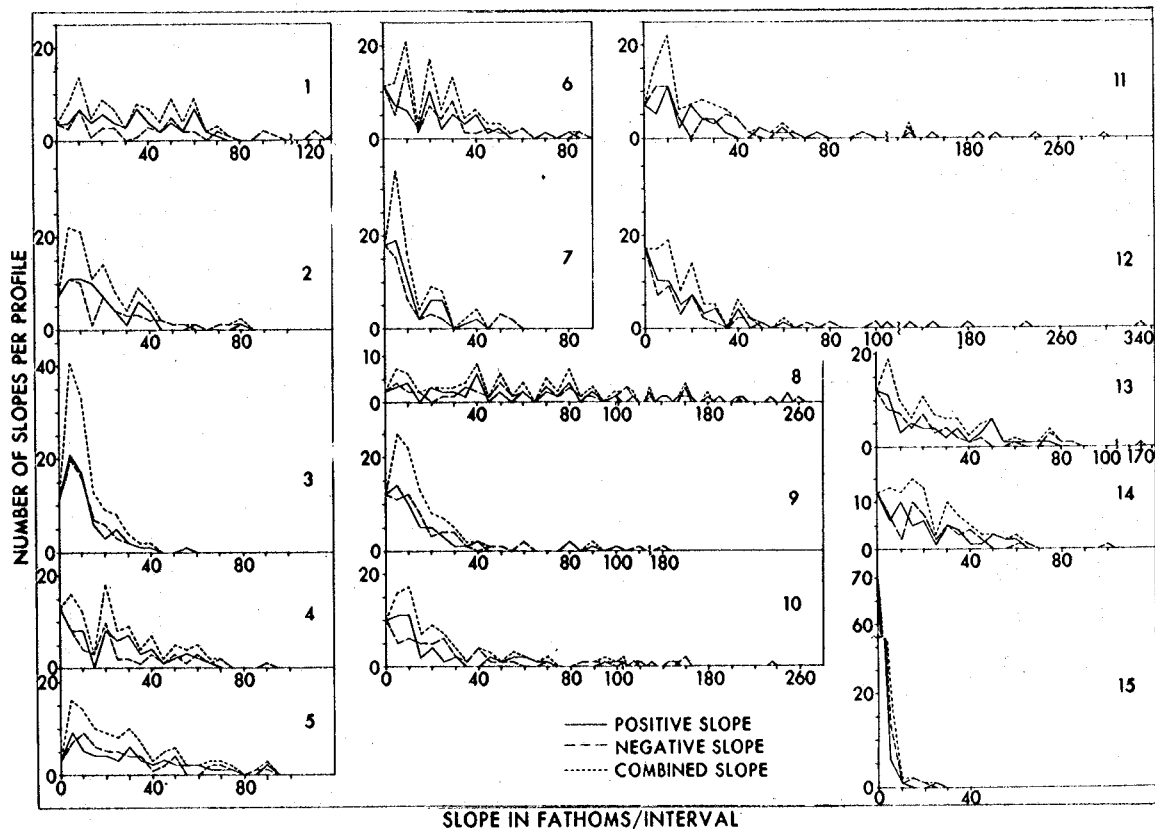
Figure 15. Slope frequency distribution of North Pacific profiles. Positive and negative slopes are facing in opposite direction (see text).

15 fm per interval (about 26 m/km), and a secondary peak near 20 fm per interval (about 35 m/km). The frequency of slopes greater than 20 fm per interval decreases more or less exponentially. The South Pacific study was carried out in part to test these discontinuities. Martynov (1958) also found a discontinuity at a slope of 25 m/km on the floor of the Kara Sea. (See table 3 for slope units.)

Probability plots of the frequency distributions of uphill (positive) and downhill (negative) sea-floor slopes of four representative profiles indicated that, although some tendency exists for normal distributions, the deviations showed that this may not be the general case. Therefore, this is tested for the South Pacific profiles.

South Pacific. The slope frequency distributions of the South Pacific profiles (figs. 16 to 20, table 8) show most of the characteristics of those from the North Pacific (fig. 15). The maxima and minima tend to fall near similar slopes. For example, a finite amount of flat slope was always present. For the combined slopes, the zero slope
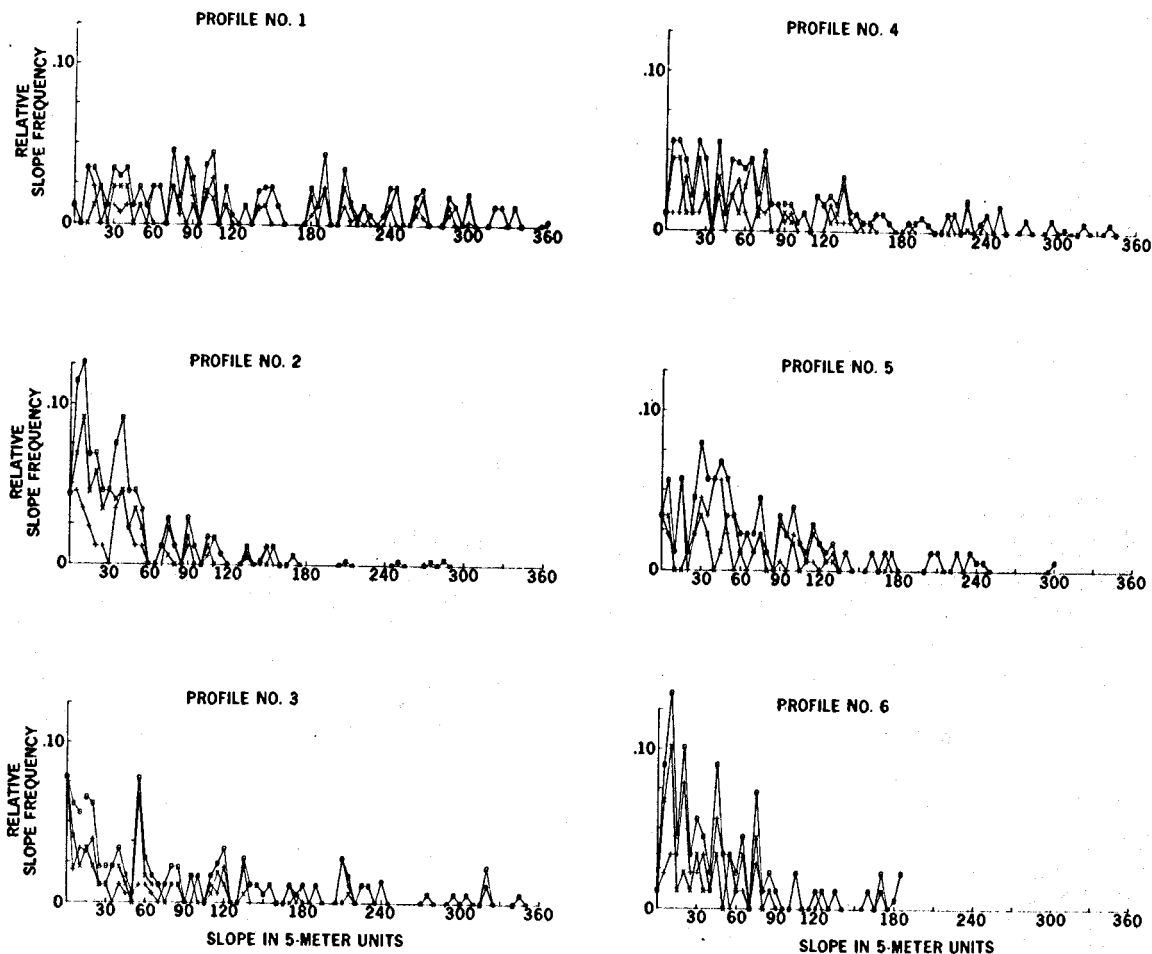
Figure 16. Slope frequency distribution of South Pacific profiles 1 to 6. Pluses are east-facing slopes, crosses are west-facing slopes, and squares are combined slopes.

($\leq$ ±2.5 m/km) represents a minimum for 24 of the 26 profiles. As in the North Pacific, the zero slope distribution for the individual positive or negative slopes is a minima or maxima depending on the individual case. The main maximum for the combined and negative slopes appears between 0 and 15 m/km in the majority of cases. The maximum of the positive slopes is more scattered but lies always between 0 and 25 m/km with more at zero slope than for the combined or negative distribution.

Most profiles show the important minimum between 20 and 30 m. This minimum is least well displayed in the positive slopes where important maxima interfere. The existance of. these minima requires maxima at steeper slopes.

The South Pacific slope distributions should show some difference from the North Pacific ones because of the lack of southern sediment.
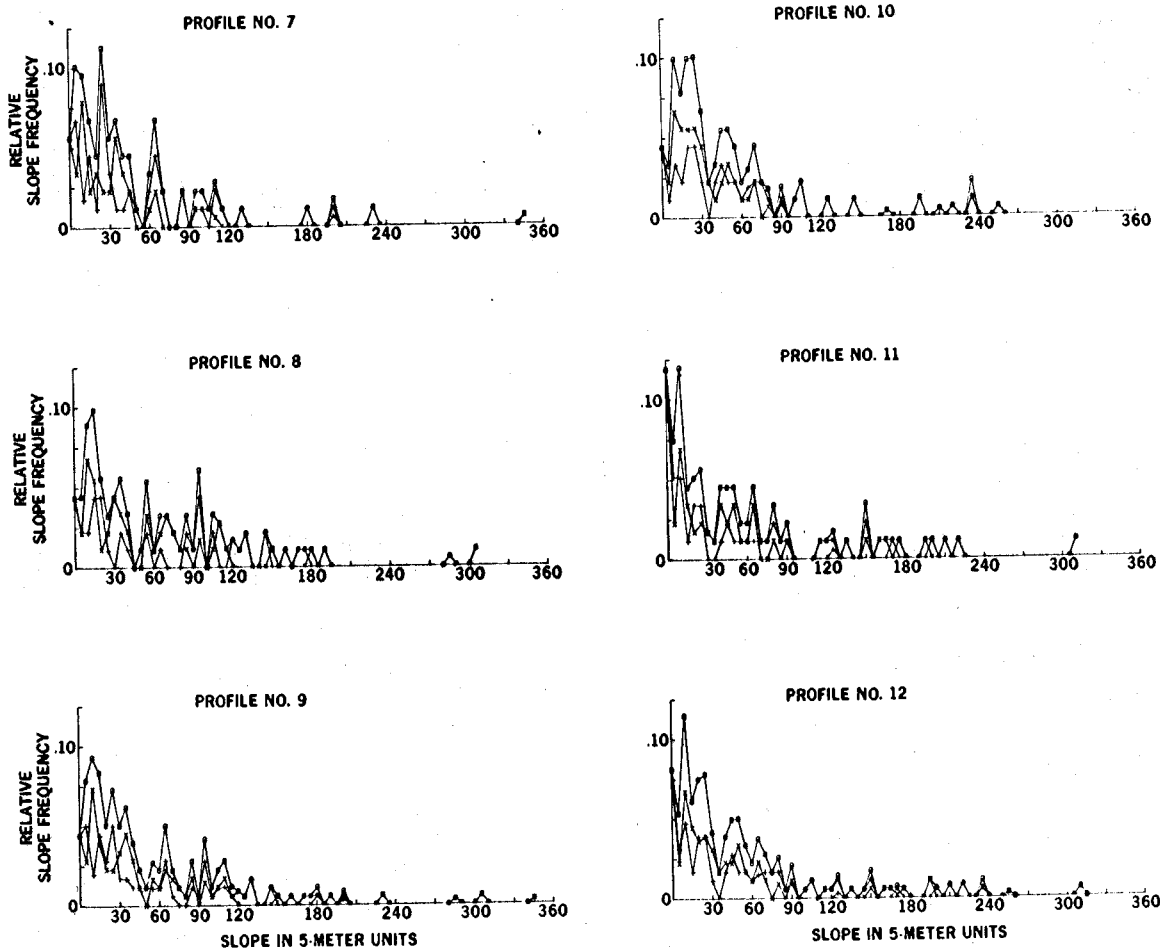
Figure 17. Slope frequency distribution of South Pacific profiles 7 to 12.

The frequency breaks in the North Pacific were interpreted to be due to sedimentary processes. The lack of South Pacific sediment would be expected to give some more scattered data with more steep slopes. Qualitatively, this seems to be the case.

As in the North Pacific, the South Pacific slope frequency distribution is a maximum for low slopes and decreases rapidly for steeper slopes. The median slope is near 40 m/km and 84 percent of the slopes are less than 125 m/km. If all profiles are combined, zero slope frequencies begin to appear at 250 m/km, and very few slopes are steeper than 450 m/km, the maximum being 920 m/km (fig. 21).

The distribution of the slopes in all of the profiles (figs. 16 through 20) is such that the geometric mean or median is a much better measure of the slope than the arithmetic mean, which is essentially meaningless (table 9).

-38-
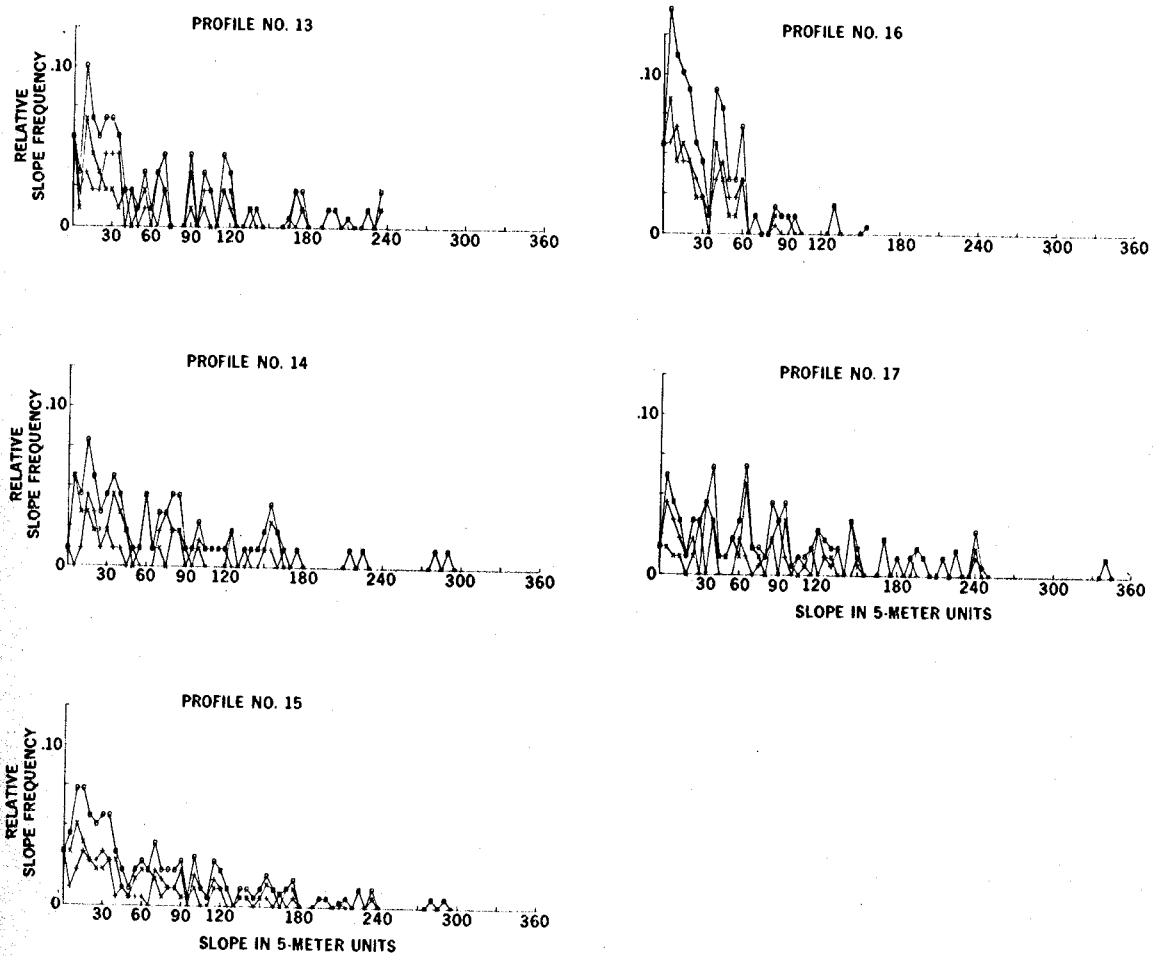
Figure 18. Slope frequency distribution of South Pacific profiles 13 to 17.

As described, slope distributions from the North Pacific are thought to be normal distributions. This hypothesis was tested for the South Pacific profiles by applying a chi square analysis to the slope frequency distributions (table 10). The distribution was arranged from the steepest negative slope (west-facing) through zero slope to the steepest positive slope (east-facing).

The mean slope of *this* distribution must be close to zero because of the canceling effect of positive and negative slopes. The mean slope is generally westward to the west of the crest of the East Pacific Rise and eastward to the east. At the postulated ancient rift, again the mean slope is westward to the west (profile 18) and eastward to the east (profile 19). The standard deviation for all profiles is large and represents the root-mean-square (rms) slope of the sea floor. The
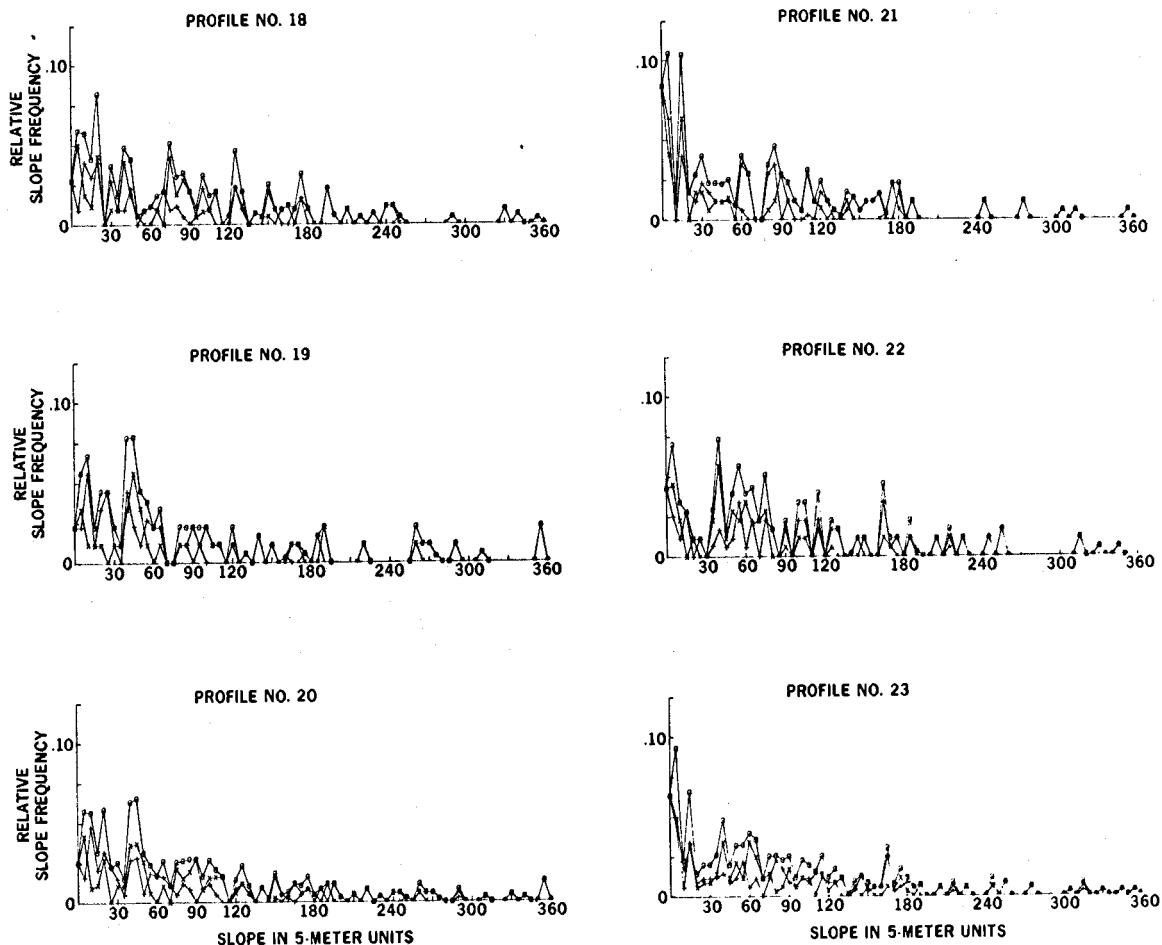
Figure 19. *Slope frequency distribution of South Pacific profiles 18 to 23.*

statistical parameters of the continuous slope distribution of the 20 unified profiles are all of moderate value: mean, 0.37 m/km; standard deviation, ± 105.2 m/km; coefficient of relative skewness, 0.704; coefficient or relative kurtosis, 7.87.

For all of the profiles, the coefficient of relative skewness is low, as indicated by near zero values of the mean slopes. The coefficient of relative kurtosis is large, which indicates one reason that the chi square values are high. However, the main reason the chi square values are high is that the curve is (1) more peaked than the normal curve, and/or is (2) significantly affected by a minimum in the zero slope. Only a few South Pacific profiles can be considered to even approach a normal distribution for slopes: profile 15* at a 5 percent level, profile 9 at a 15 percent level, profile 10 at a 40 percent level,

PROFILE NO. 24

PROFILE NO. 25
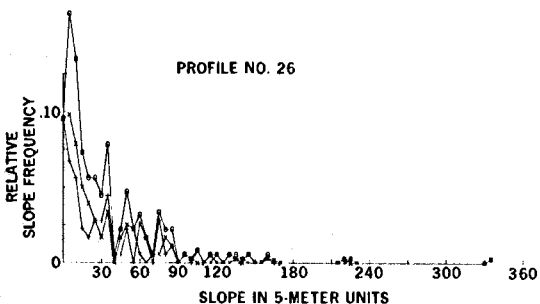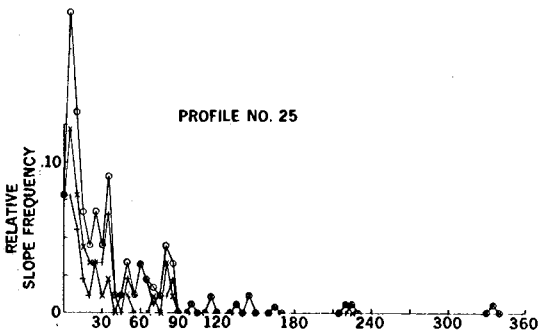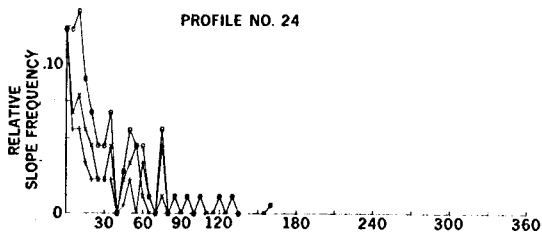
Figure 20. Slope frequency distri-
  bution of South Pacific profiles,
  24 to 26.

PROFILE NO. 26

SLOPE IN 5-METER UNITS

and profile 12 at a 40 percent level. Significantly, the 200-km profiles have a more normal distribution. This is confirmed by combining all twenty 111-km profiles (fig. 21). This yields a chi square value of 38.2 for a percentile of less than 2.5 percent, a very good normal distribution over long profiles, but that for 100-km profiles, a log-normal or some other distribution describes the distribution better for slopes all facing a given direction.

The cumulative slope plot of the 20 unified profiles shows a similar linear character as do the cumulative slope plots of the single profiles (fig. 21). The parameters for m and $\log_{10}k$, respectively, of the

Table 8. *South Pacific Slopes Not Plotted on Slope Frequency Diagrams (Figures 16-20).*

Profile	East Facing		West Facing	
	Percent Frequency	Slope (m/km)	Percent Frequency	Slope (m/km)
1	1.0	420	0.6	415
	0.6	450	0.6	430
	0.2	465	0.9	475
2			0.6	375
3	1.1	375	0.2	670
	0.4	530	0.2	920
4			1.1	400
			0.3	555
			0.2	825
10*	0.3	485		
14*			1.1	375
17			1.1	500
18	0.3	485	0.3	380
	0.3	625	0.9	500
19	1.1	370	1.1	370
	1.1	415	0.6	375
			1.1	465
21*	1.2	370	0.2	395
	0.6	375	0.6	610
22*	1.2	425	0.2	385
	0.6	435	1.1	410

* Profiles 12, 15, 20, and 23 contain the same slopes as, respectively, profile 10, 14, 18 and 19, and 21 and 22 but with half the frequency because they are twice as long.
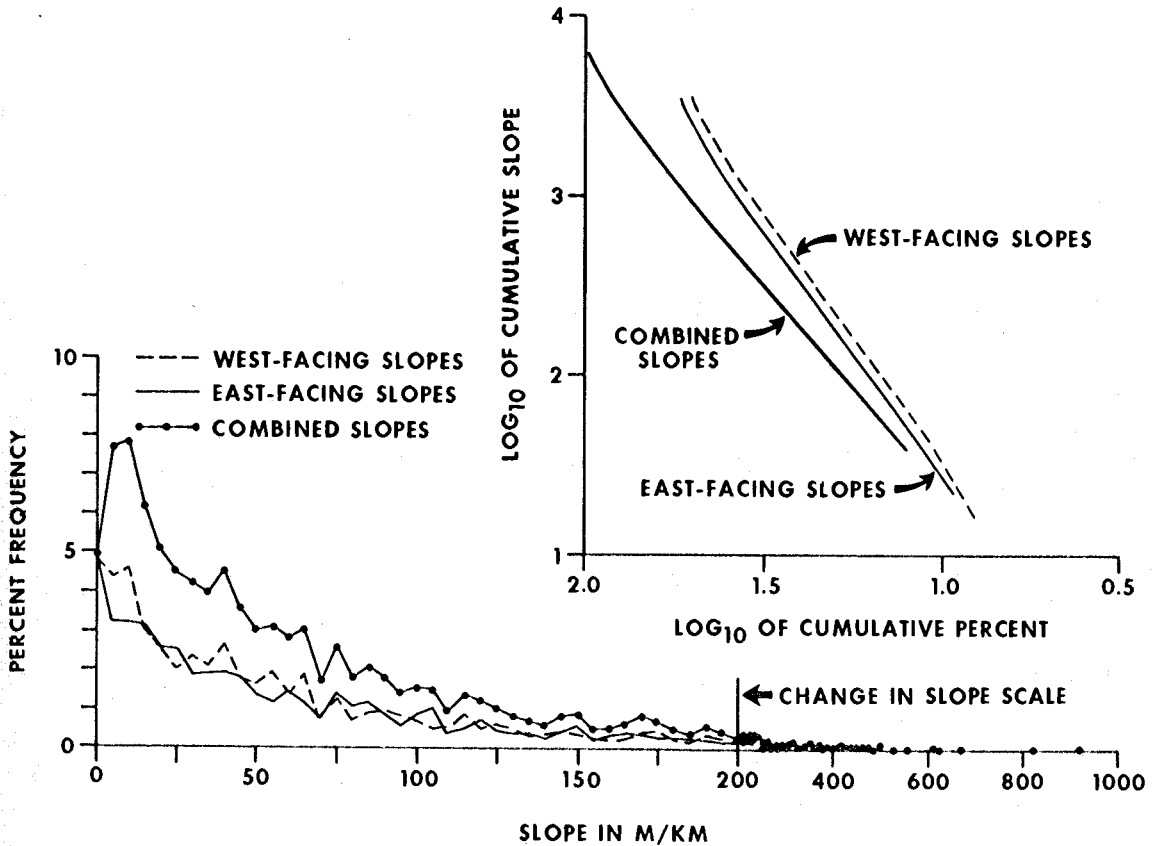
Figure 21. Slope distribution of 20 combined profiles, South Pacific.

unified plot are east-facing, 2.70; west-facing, 2.67; and combined, 2.31. The statistical parameters of the continuous unified distribution are mean, 0.37 m/km; deviation, ± 105.2 m/km; coefficient of relative skewness, 0.704; coefficient of relative kurtosis, 7.87.

5.3 Cumulative Distribution of Slopes

North Pacific. The cumulative frequency plots (fig. 22) fall on nearly straight lines that are characteristic of the profile. Some of the plots may be approximated by two straight lines, one for the lower part and one for the upper part. The profiles may legitimately be divided into two parts where necessary, because the steeper portions represent seamounts or escarpments that have a separate geologic origin from the rest of the profile. As already mentioned, such a straight line on log-log graph paper is represented by equations (18) or (19):

$$y = k\, x^m$$

or

$$\log_{10} y = m \cdot \log_{10} x + \log_{10} k$$

where y is the cumulative elevation (or depth), x is the cumulative frequency (or cumulative intervals), and k and m are parameters.

Each profile yielded one or more sets of parameters m and k, which are adjusted as described in section 4.

Revised parameters k and m are plotted (fig. 23) on semilog paper and are shown to be related to one another (dependent variables). They fall along two straight lines, one for the individual uphill and downhill plots and one for the plots of the combined uphill-downhill plots; they are related by

$$m = -0.533 \log_{10} k + 1.85; \qquad\qquad\qquad (26)$$

for the combined plots, they are related by

$$m = -0.430 \log_{10} k + 1.78 . \qquad\qquad\qquad (27)$$

It was this striking relationship that the South Pacific study is designed to test.

A decrease of k and m represents a numerical increase of the gentle slopes and a numerical decrease of the steeper slopes, thus representing a more subdued bathymetry.

A classification of the sea floor based on m (or k) could be easily made and would be quantitative. This is not done here, although it will be useful geographically.

South Pacific. The log-log plots of the cumulative slope ("depth") versus cumulative percent approach linearity as expected (figs. 24 through 28). Percent frequency is used in the plots for easy comparison to the North Pacific data. For relative frequency, the plots are exactly the same but the logarithmic coordinates are each reduced by two. These plotted straight lines have equations (18) and (19). As shown in section 4, each profile has a series of parameter sets m and $\log_{10} k$, where $\log_{10} k$ differs if the frequency is relative or percent. Both sets of $\log_{10} k$ have been calculated, one for the North Pacific comparison and one for the simplest relations. We shall first make the North Pacific comparison with percent frequency. In most cases for percent

Table 9. Mean Slope of the Combined Slopes and Standard Deviation, South Pacific. (Note that the arithmetic mean is almost without meaning.)

Profile	Median (m/km)	Geometric Mean (m/km)	Arithmetic Mean (m/km)
1	103	98.7 ± 12.6	141.2 ±108.5
2	28	27.1 ± 12.2	42.6 ± 49.5
3	53	47.6 ± 16.6	90.8 ±104.4
4	62	59.5 ± 13.2	92.7 ± 92.5
5	47	47.9 ± 12.1	68.7 ± 58.3
6	33	33.0 ± 11.6	48.0 ± 44.4
7	27	28.8 ± 12.6	45.8 ± 50.4
8	41	40.5 ± 13.1	62.8 ± 57.5
9*	32	34.2 ± 13.0	54.2 ± 54.9
10	28	32.6 ± 11.9	49.5 ± 56.2
11	36	30.3 ± 15.53	56.7 ± 63.2
12*	34	31.2 ± 13.7	52.8 ± 59.8
13	35	39.5 ± 13.6	63.6 ± 60.7
14	59	51.4 ± 12.5	76.8 ± 69.8
15*	45	45.0 ± 13.2	70.0 ± 65.7
16	20	22.0 ± 11.2	31.4 ± 28.2
17	66	60.6 ± 13.0	90.8 ± 81.5
18	72	57.1 ± 14.3	93.1 ± 92.1
19	51	57.9 ± 14.5	100.1 ±108.2
20*	61	58.2 ± 14.3	96.8 ±100.2
21	56	43.3 ± 16.5	81.4 ± 91.1
22	65	60.8 ± 14.5	98.0 ± 92.7
23*	60	50.4 ± 15.7	88.7 ± 92.2
24	17	19.3 ± 12.5	30.6 ± 30.7
25	17	20.2 ± 12.7	34.2 ± 43.5
26*	18	20.2 ± 12.7	33.5 ± 39.15

Table 10. Statistical Parameters for Slopes of Entire Profile, South Pacific. (Chi square value has 59 degrees of freedom.)

Profile	Mean and Standard Deviation		Relative Coefficient		Chi Square	
			skewness	kurtosis	value	percentile
1	0.4	± 178.0	-0.33	2.9	95.9	99.9
2	-2.0	± 65.2	0.96	10.9	66.1	80.
3	-0.03	± 138.3	0.83	9.1	121.1	99.95+
4	-0.03	± 131.0	1.04	7.7	88.2	99.5
5	-0.5	± 90.1	-0.40	3.9	72.3	90.
6	-1.8	± 65.4	-0.71	4.2	80.1	97.5
7	1.2	± 68.1	-0.99	7.8	75.5	95.
8	-0.003	± 85.1	-0.48	4.4	74.5	95.
9*	-0.2	± 77.1	-0.74	5.6	46.7	15.
10	-0.1	± 74.9	-0.99	10.6	53.5	40.
11	0.9	± 84.9	0.89	5.0	95.8	99.9
12*	0.5	± 79.8	0.27	7.3	54.4	40.
13	0.9	± 87.9	-0.50	3.7	79.5	97.5
14	1.6	± 103.8	0.92	4.5	77.0	95.
15	0.3	± 96.0	0.78	4.4	40.4	5.
16	-0.9	± 42.2	-0.65	4.3	102.6	99.95
17	-0.7	± 122.03	0.84	5.4	99.5	99.95
18	-0.6	± 131.0	0.59	6.1	89.5	99.5
19	1.0	± 147.4	0.74	4.7	118.5	99.95+
20	-0.8	± 139.3	0.71	5.4	78.6	97.5
21	1.7	± 122.2	0.86	7.3	124.0	99.95+
22	0.7	± 134.9	-0.38	4.6	97.6	99.9
23*	2.2	± 127.9	0.62	5.9	74.2	95.
24	1.8	± 43.3	0.92	4.3	91.8	99.9
25	-0.04	± 55.4	-1.12	12.1	87.4	99.5
26*	-0.2	± 51.5	-0.88	9.8	57.6	50.0
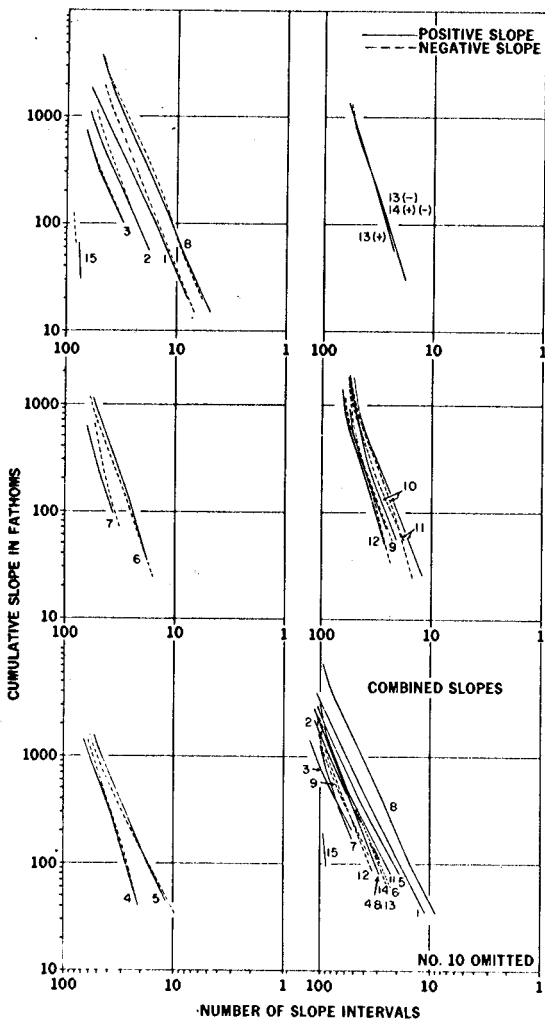
Figure 22. Cumulative slope distribution, North Pacific. Combined plot of profile 10 is omitted because it falls on all or part of the traces of profiles 2 and 11.

frequency, the parameter sets have an initial moderate magnitude (gentlest slope sets), which then pass through a minimum and become high for the steeper slope sets. Generally the parameters lie along a smooth line. The only significant departures are for profiles 1, 20*, 22, and 23*. In some profiles, the west-facing and east-facing parameter sets lie along (or almost along the same line: 6, 7, 11, 13, 16, 20*, and 21. The maximum cumulative values for each profile are given in table 11.

For comparison, we selected a decade parameter set, $\log_{10}k$ and m, that best characterized each profile from the series of decade parameter sets calculated for each profile. Generally, the first or second decade parameter set is used, because the m, $\log_{10}k$ line here is generally straight. The first decade parameter set represents, in general, about 50 percent of the slopes, although it can represent as much as 82 percent as in profile 25 where the relief is small. In 15 out of 78 cases, the·
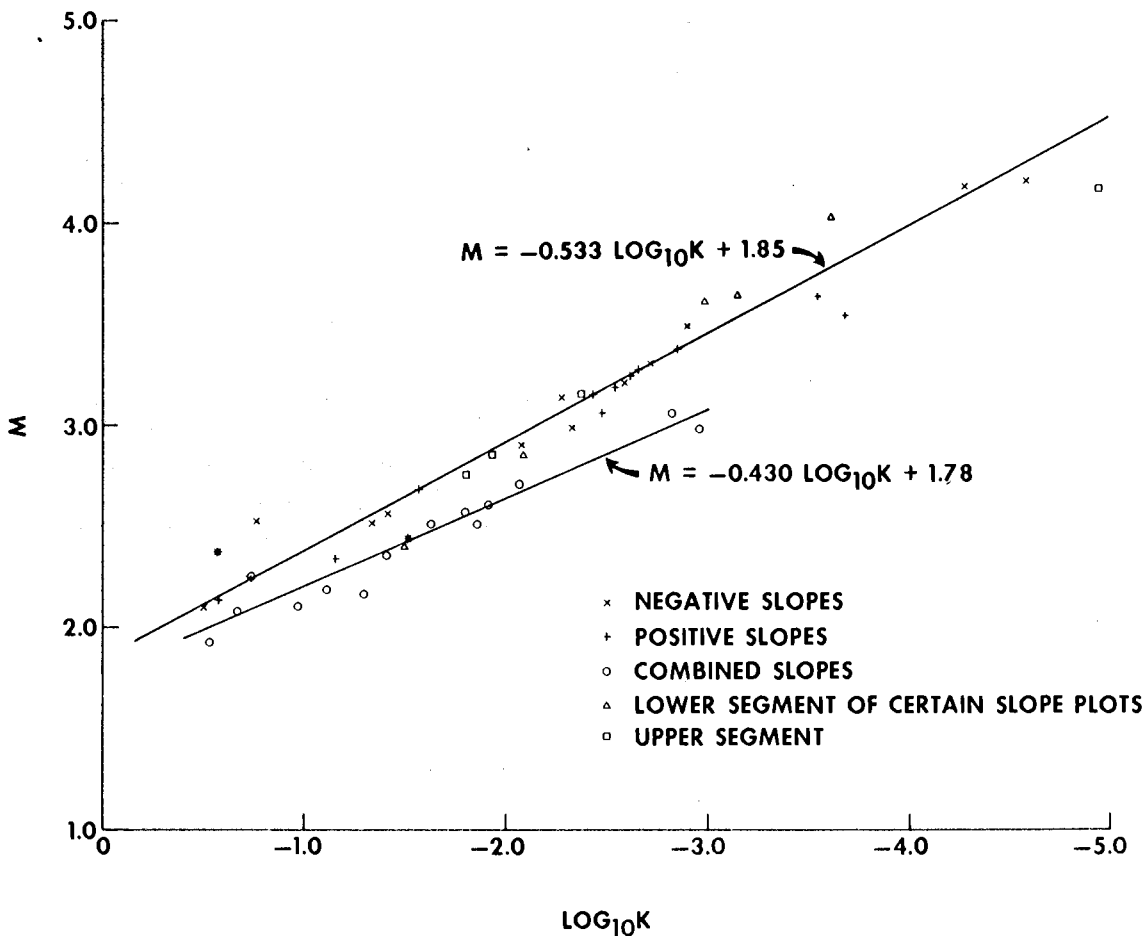
Figure 23. Parameters m versus $\log_{10}k$, North Pacific, for all or most of each profile. In addition, parameters are presented for major positive or negative straight segments of profiles 3, 4, 6, and 10 (see fig. 22). Parameters for profile 15 are too large to be plotted and are for m and $\log_{10}k$, respectively, positive: 21.5, -41.5; negative, 13.1, -24.0; combined: 10.5, -21.0.

line is better characterized by two segments; thus, two parameter sets are selected as follows. In several cases the first selected parameter set represents rather less than 50 percent. In such cases another portion of curve is also straight. In all cases where the initial selected parameter represents less than 35 percent (only one, 17 percent, is chosen less than 20 percent), a second parameter set can be and is chosen for the straight line representing higher slopes. The total then represented in every case more than 50 percent of the slopes. In certain other cases, two parameter sets, for two straight line segements, are
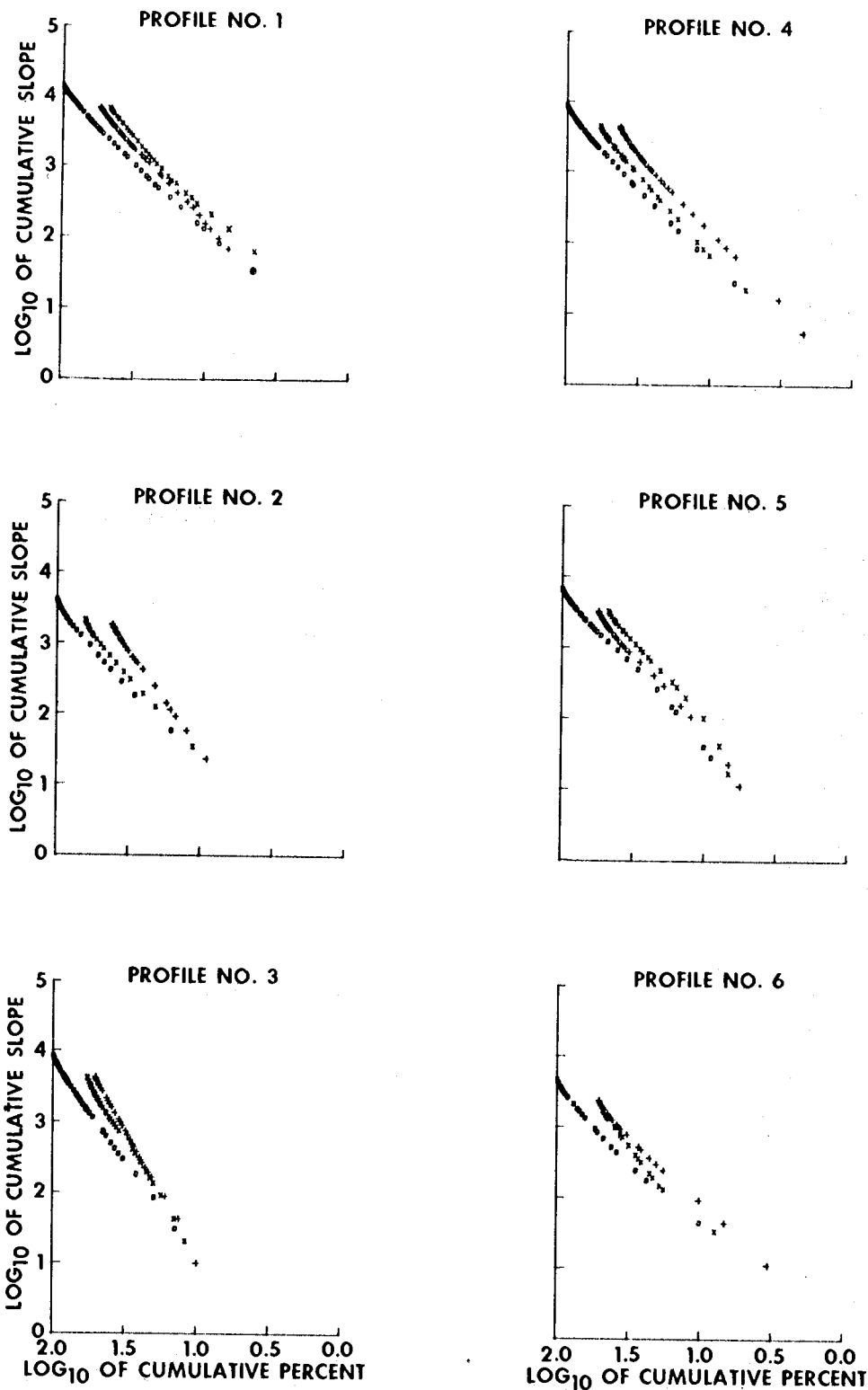
Figure 24. Cumulative slope distribution of South Pacific profiles 1 to 6.
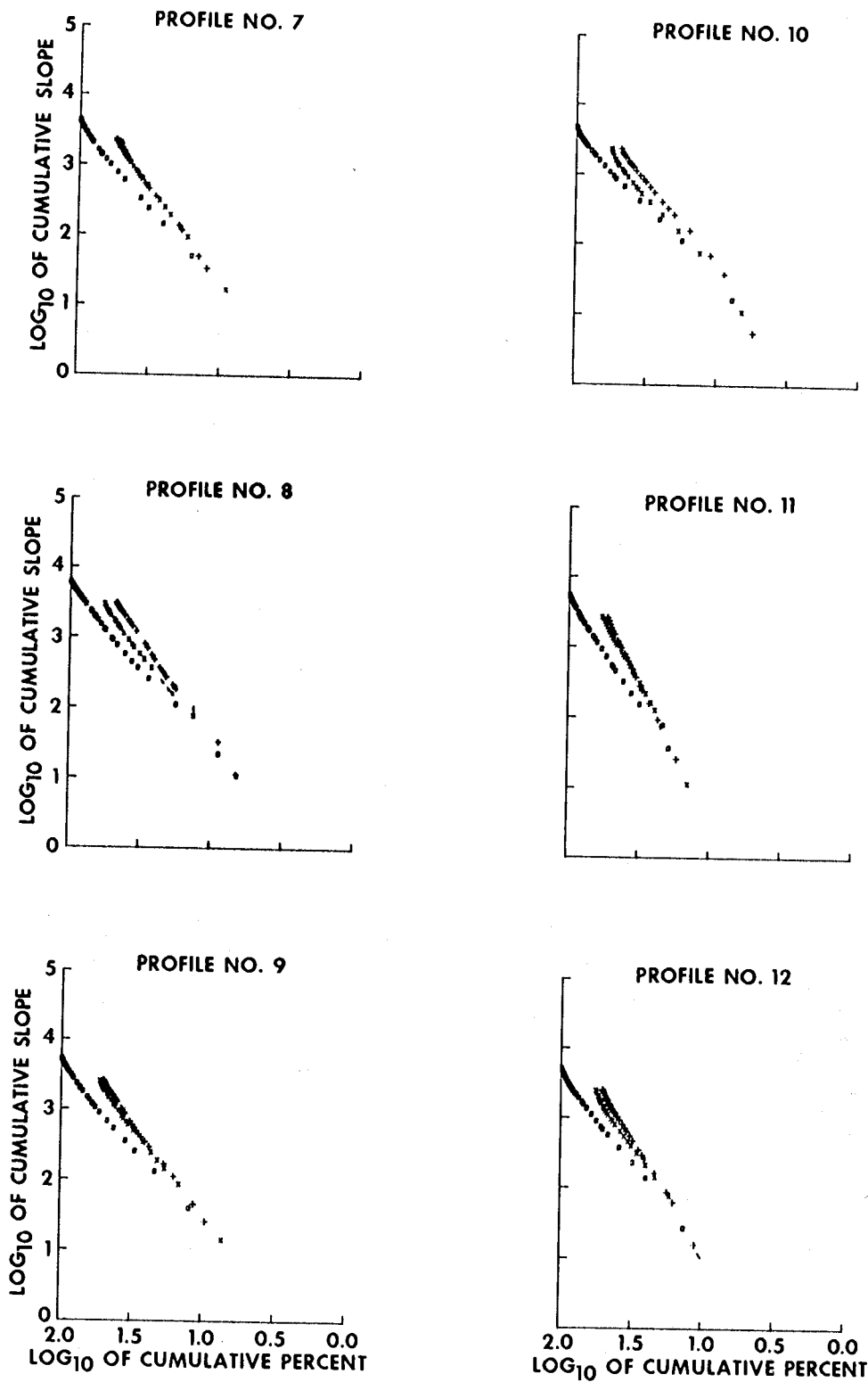
Figure 25. Cumulative slope distribution of South Pacific profiles 7 to 12.
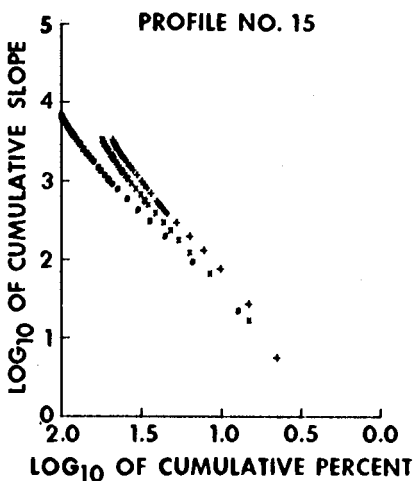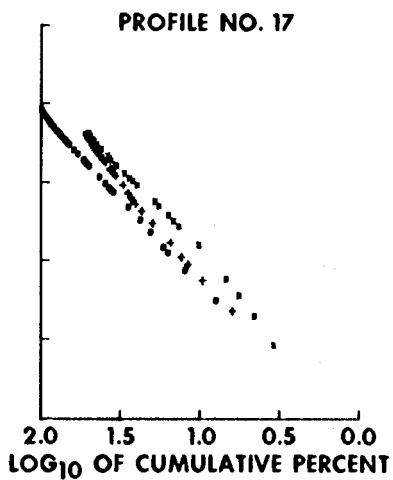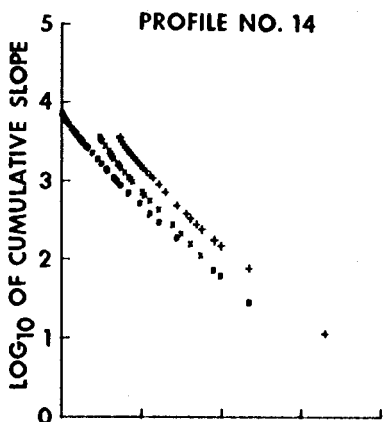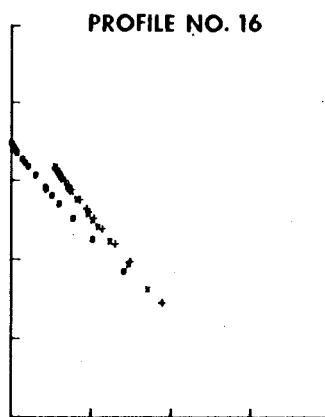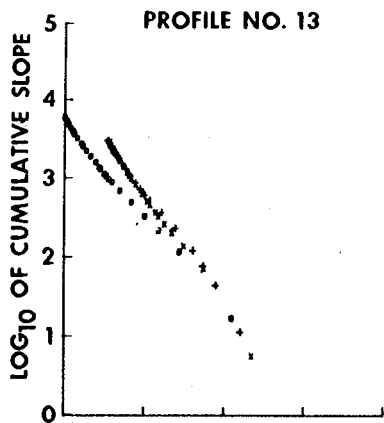
Figure 26. Cumulative slope distribution of South Pacific profiles 13 to 17.
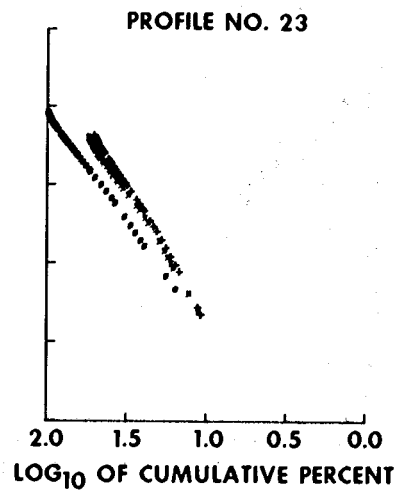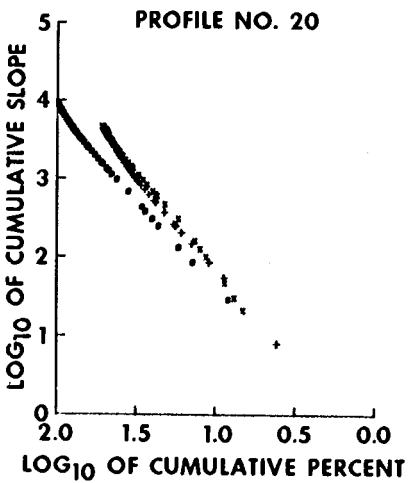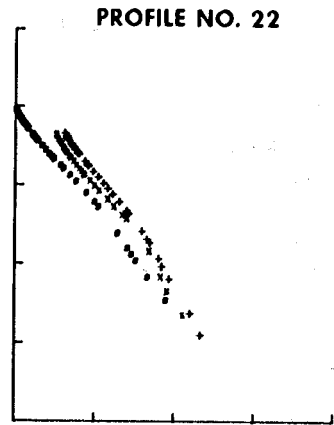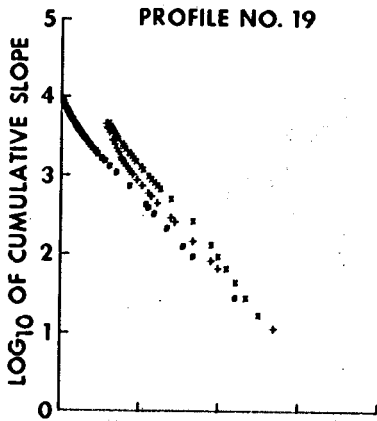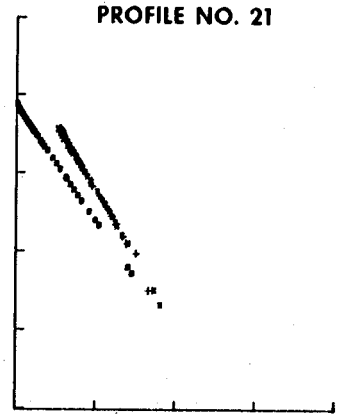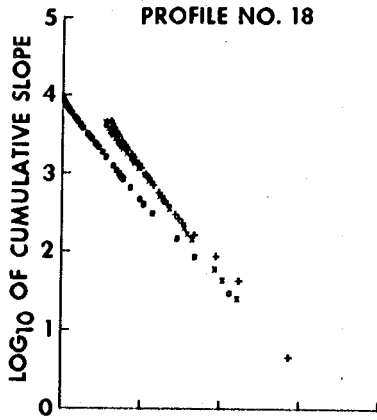
Figure 27. Cumulative slope distribution of South Pacific profiles 18 to 23.

PROFILE NO. 24

PROFILE NO. 26

PROFILE NO. 25
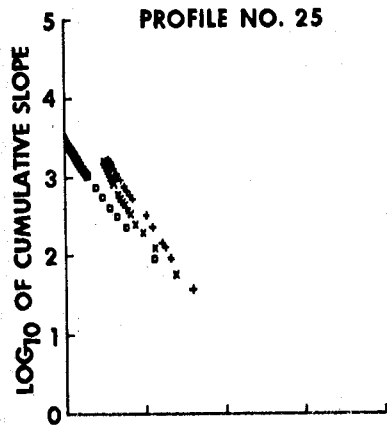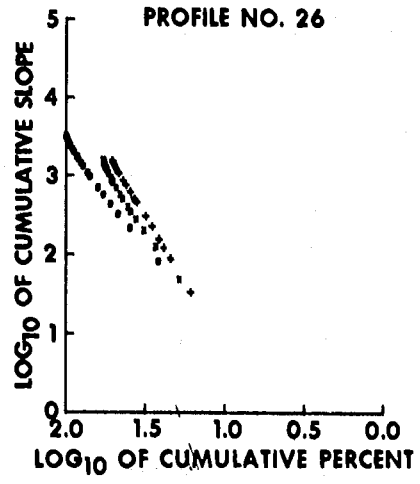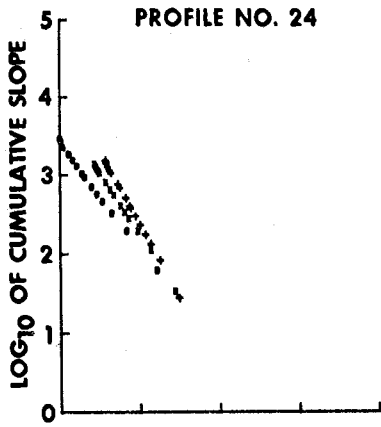
Figure 28. Cumulative slope distribution of South Pacific profiles 24 to 26.

required even where the first one represents one-third to one-half of the slopes; in such cases, the two parameter sets represent over 70 percent of the slopes.

The selected parameter sets, m and $\log_{10} k$, are seen to be linearly related (fig. 29). Least squares parameters are calculated (fig. 29). These parameters and errors, especially the multiple correlation coefficient (0.947 to 0.961), indicate a strong dependence between m and $\log_{10} k$. The difference between the relations of the west-facing slopes, the east-facing slopes, and that of the collected east- and west-facing slopes is not statistically significant. The combined relation is satisfyingly linear and different from the others.

This experiment was designed to test the striking North Pacific discovery that the cumulative slope plots tend to linearity and that the derived parameters m and $\log_{10} k$ are themselves dependent variables as shown by (26) and (27).

Table 11. *Hand-Selected Characteristic Decade Parameters, m and $\log_{10}k$, Using Relative Frequency.*

| | Type of Bottom Slope Compilation | | | | | |
Profile	East Facing m	$\log_{10}k$	West Facing m	$\log_{10}k$	Combined m	$\log_{10}k$
1	+2.01	+2.28	+1.82 2.24	+2.24 2.55	+2.41	+2.13
2	2.84	2.33	2.26	1.68	2.27	1.50
3	3.78	2.80	3.52 2.89	2.61 2.23	2.76	1.84
4	2.03	2.23	2.15	2.04	2.12	1.83
5	2.42	2.06	2.26	2.22	2.19	1.76
6	1.88	1.82	2.65	2.09	2.09	1.56
7	2.75	2.02	2.65	1.99	2.26	1.52
8	2.89	2.46	2.53	2.03	2.19	1.65
9*	2.66	2.12	2.48	1.97	2.17	1.56
10	2.36	2.07	2.13	1.76	1.96	1.54
11	3.97	2.48	3.35	2.17	2.92	1.65
12*	3.07	2.24	2.65	1.93	2.36	1.57
13	2.89	2.25	3.01	2.27	2.31 3.07	1.65 1.79
14	2.24	2.34	2.24	2.00	1.93 2.66	1.70 1.85
15*	2.68	2.35	2.38	2.02	2.05 2.61	1.66 1.79
16	2.54	1.86	2.65	1.88	2.25	1.44
17	2.38	2.21	2.40	2.44	2.17	1.87
18	2.59	2.36	2.73	2.42	2.18	1.79
19	2.21	2.03	2.56	2.42	2.10	1.76
20*	2.36	2.17	3.01 2.32	2.84 2.25	2.20	1.81
21	3.64	2.60	3.66 2.96	2.62 2.30	2.96	1.86
22	3.61 2.38	3.34 2.36	2.22	2.11	2.96 2.15	2.28 1.87

| Profile | Type of Bottom Slope Compilation | | | | | Log$_{10}$ k |
| | East Facing | | West Facing | | Combined | |
	m	Log$_{10}$ k	m	Log$_{10}$ k	m	
23*	3.69	2.92	3.75	2.94	2.87	1.98
	2.97	2.48	2.70	2.24	2.56	1.86
24	3.80	2.28	3.21	1.84	2.55	1.35
					3.00	1.46
25	3.01	2.02	3.03	1.90	2.50	1.39
					3.29	1.48
26*	3.33	2.15	2.98	1.81	2.32	1.27
					2.83	1.45

The relationship is firmly verified in the South Pacific where the equations for the opposite facing slopes is

$$m = -0.557 \log_{10} k + 2.04 , \tag{28}$$

and for the combined plots it is

$$m = -0.473 \log_{10} k + 1.88 . \tag{29}$$

Thus we have shown that the North Pacific and South Pacific data represent the same properties. Let us look more closely at the slope properties using South Pacific relative frequency.

For relative frequency, parameter m and its variation are the same as for percent frequency. However, the variation of parameter $\log_{10}k$ is very small — a great contrast. As a consequence, the results are much easier to interpret. A characteristic parameter set for each profile is selected in three ways which give similar sets: (1) one parameter set (sometimes two) is hand-selected at the same decade frequency for which the percent parameter was hand-selected (table 12); (2) one parameter set is selected by calculating the mean and standard deviation for each successive slope frequency and using a weighting factor of the frequency squared (table 13); and (3) one parameter set is selected by calculating the mean and standard deviation of the decade parameters using a weighting factor of the decade frequency cubed (table 13, figs. 30 and 31).

$M_W = -0.522 \, LOG_{10}K + 2.07$

$M_E = -0.584 \, LOG_{10}K + 2.02$

$M_C = -0.473 \, LOG_{10}K + 1.88$

× WEST-FACING SLOPES
+ EAST-FACING SLOPES
○ COMBINED

$LOG_{10}K$
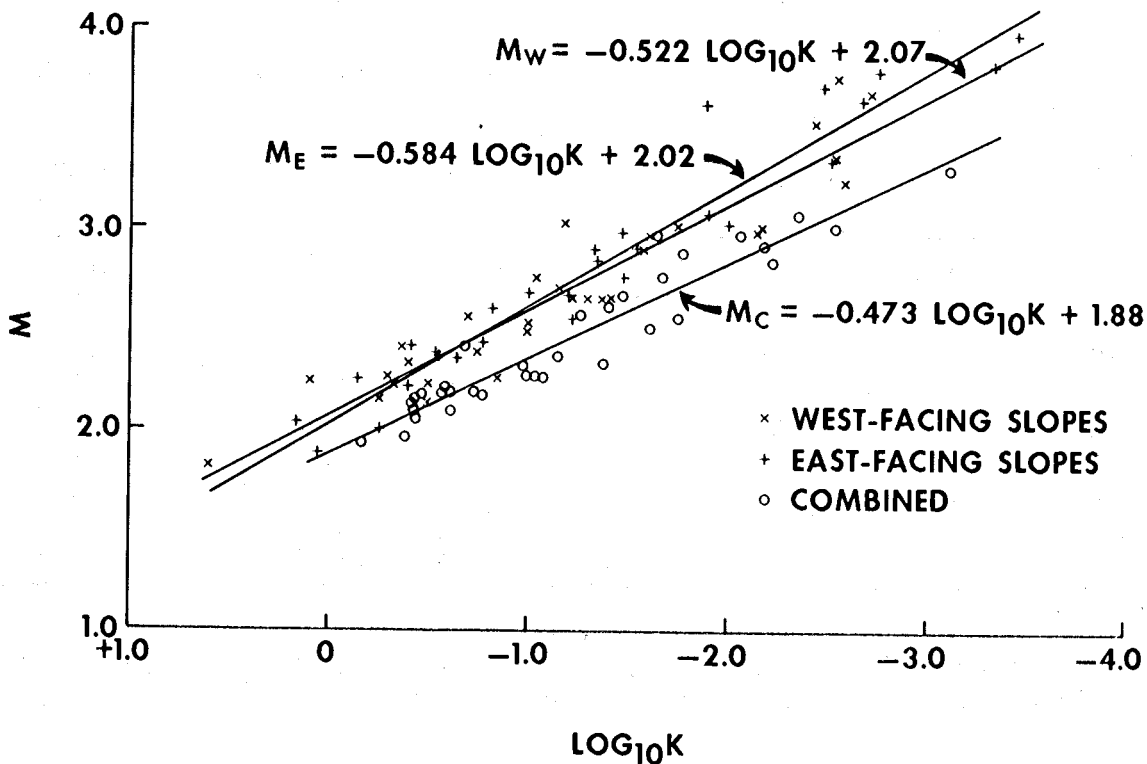
Figure 29. Decade parameters m and $log_{10}k$, South Pacific, using percent frequency.

Several features stand out. First, the selected parameter sets are all similar and thus either hand or machine selection is suitable. Next, the standard deviation of the decade parameters is less than that for each data point, thus the decade parameters are preferred. The hand-chosen parameters fall within the standard deviation of almost all of the parameters from successive data points and of most of the decade parameters. Where two hand-chosen parameter sets are used for a profile, the machine-chosen parameters are intermediate in value with suitable deviations. Especially striking are the small deviations of decade $log_{10}k$ (table 13, fig. 31), which are always less and are generally much less than those of decade parameter m.

The cumulative slope plot of the 20 unified profiles (fig. 21) shows a similar linear character as the cumulative slope plots of the single profiles. The machine-chosen, weighted decade parameters for m and $log_{10}k$ of the unified plot using relative frequency are, respectively, east-facing, 2.74, 2.24; west-facing, 2.72, 2.14; and combined, 2.43, 1.70.

Table 12. Cumulative Depth and Percent, South Pacific

Profile	Cumulative Depth (m)			Cumulative Percent		
	West-Facing	East-Facing	Combined	West-Facing	East-Facing	Combined
1	7037	7078	14115	46.8	54.3	100
2	2228	2031	4259	63.3	41.1	100
3	4541	4537	9078	57.6	50.3	100
4	4635	4638	9273	58.6	42.4	100
5	3459	3407	6866	47.7	55.8	100
6	2310	2492	4802	50.0	51.1	100
7	2230	2349	4579	50.6	55.1	100
8	3138	3138	6276	57.3	47.1	100
9*	2699	2722	5421	53.7	50.8	100
10	2481	2471	4952	56.3	48.2	100
11	2788	2879	5667	58.5	53.4	100
12*	2619	2665	5284	57.1	51.1	100
13	3134	3226	6360	52.3	53.3	100
14	3761	3921	7682	57.9	43.2	100
15*	3489	3514	7003	55.7	47.7	100
16	1616	1525	3141	52.9	52.7	100
17	4573	4508	9081	50.1	51.6	100
18	4685	4628	9313	53.8	49.0	100
19	4955	5058	10013	50.0	52.3	100
20*	4882	4801	9683	52.5	50.0	100
21	3988	4155	8143	55.4	53.0	100
22	4863	4934	9797	55.4	48.9	100
23*	4323	4543	8866	55.4	51.0	100
24	1439	1620	3059	60.7	51.7	100
25	1714	1710	3424	54.2	53.6	100
26*	1683	1663	3346	58.3	51.2	100

Table 13. *Means and Standard Deviation of Parameters m and $Log_{10}k$ Using Relative Frequency and Weighting Factors*

	Type of Bottom Slope Compilation					
Profile	East Facing		West Facing		Combined	
	m	$Log_{10}k$	m	$Log_{10}k$	m	$Log_{10}k$
1[1]	2.16±.32	2.33±.18	2.14±.30	2.45±.22	2.10±.27	2.04±.10
1D[2]	2.14±.16	2.34±.07	2.19±.20	2.51±.13	2.09±.20	2.06±.05
2	2.88±.46	2.36±.23	2.33±.38	1.67±.10	2.25±.38	1.45±.08
2D	2.86±.11	2.35±.05	2.39±.21	1.72±.07	2.34±.07	1.51±.03
3	3.62±.67	2.78±.55	3.24±.53	2.41±.27	2.85±.37	1.86±.12
3D	3.59±.14	2.70±.07	3.14±.24	2.33±.09	2.82±.22	1.85±.03
4	2.29±.47	2.38±.26	2.29±.33	2.07±.19	2.19±.36	1.80±.10
4D	2.23±.28	2.35±.15	2.31±.14	2.12±.05	2.16±.19	1.83±.03
5	2.26±.44	2.06±.27	2.41±.56	2.37±.51	2.14±.33	1.79±.15
5D	2.25±.20	2.01±.07	2.31±.22	2.25±.12	2.11±.17	1.75±.03
6	1.97±.35	1.83±.17	2.19±.66	1.72±.40	2.07±.44	1.47±.14
6D	2.00±.20	1.89±.09	2.62±.30	2.08±.14	2.20±.24	1.58±.04
7	2.71±.34	2.02±.16	2.75±.53	2.06±.19	2.38±.39	1.52±.04
7D	2.73±.15	2.03±.06	2.73±.21	2.05±.09	2.41±.23	1.55±.03
8	2.75±.39	2.38±.33	2.59±.42	2.07±.23	2.32±.35	1.66±.13
8D	2.86±.09	2.43±.04	2.56±.14	2.04±.05	2.42±.23	1.71±.05
9*	2.72±.32	2.16±.18	2.57±.36	2.03±.16	2.31±.34	1.57±.07
9D*	2.77±.22	2.18±.10	2.57±.22	2.02±.08	-2.37±.26	1.61±.05
10	2.56±.64	2.27±.58	2.37±.62	1.89±.30	2.12±.45	1.57±.13
10D	2.45±.22	2.11±.10	2.33±.28	1.83±.10	2.12±.21	1.56±.02
11	4.12±.47	2.54±.18	3.97±.80	2.58±.52	3.02±.33	1.67±.05
11D	4.04±.14	2.51±.06	3.50±.28	2.23±.10	3.01±.23	1.66±.02
12*	3.33±.53	2.43±.33	3.12±.65	2.25±.45	2.54±.35	1.63±.11
12D*	3.14±.20	2.27±.08	2.87±.27	2.01±.09	2.50±.19	1.59±.02
13	2.76±.54	2.26±.40	3.10±.61	2.44±.50	2.46±.40	1.71±.14
13D	2.72±.19	2.20±.07	2.95±.27	2.26±.12	2.50±.31	1.69±.06
14	2.12±.53	2.19±.33	2.36±.34	2.02±.16	2.15±.39	1.72±.11
14D	2.16±.20	2.29±.11	2.34±.22	2.05±.09	2.20±.26	1.77±.06

| Profile | Type of Bottom Slope Compilation | | | | | |
| | East Facing | | West Facing | | Combined | |
	m	$Log_{10}k$	m	$Log_{10}k$	m	$Log_{10}k$
15*	2.52±.53	2.33±.50	2.52±.31	2.07±.15	2.24±.34	1.69±.09
15D*	2.52±.22	2.27±.11	2.53±.23	2.09±.09	2.28±.25	1.71±.06
16	2.56±.18	1.87±.08	2.74±.34	1.89±.13	2.33±.27	1.40±.06
16D	2.57±.07	1.88±.03	2.74±.12	1.92±.05	2.40±.15	1.45±.01
17	2.57±.48	2.27±.22	2.14±.35	2.28±.24	2.25±.33	1.87±.08
17D	2.58±.14	2.32±.06	2.10±.18	2.24±.10	2.24±.14	1.89±.02
18	2.64±.51	2.42±.41	2.68±.27	2.37±.12	2.36±.33	1.82±.11
18D	2.65±.23	2.39±.12	2.65±.11	2.36±.05	2.44±.18	1.88±.05
19	2.54±.79	2.15±.32	2.37±.53	2.33±.31	2.32±.57	1.79±.10
19D	2.45±.54	2.14±.23	2.40±.23	2.33±.11	2.23±.33	1.79±.05
20*	2.55±.52	2.28±.24	2.48±.37	2.36±.23	2.31±.36	1.82±.07
20D*	2.47±.35	2.22±.16	2.45±.18	2.32±.09	2.28±.19	1.83±.03
21	3.80±.54	2.71±.29	3.45±.43	2.53±.21	2.99±.28	1.86±.03
21D	3.61±.11	2.58±.05	3.33±.23	2.46±.10	2.97±.12	1.86±.01
22	2.77±.48	2.61±.34	2.72± 68	2.42±.44	2.45±.42	1.97±.17
22D	2.65±.27	2.50±.16	2.61±.30	2.28±.12	2.38±.22	1.93±.05
23*	3.34±.47	2.72±.30	3.09±.50	2.46±.26	2.75±.29	1.92±.07
23D	3.20±.27	2.60±.15	3.01±.28	2.39±.14	2.70±.16	1.90±.04
24	3.82±.26	2.30±.13	3.23±.25	1.87±.13	2.75±.26	1.40±.04
24D	3.78±.07	2.28±.03	3.18±.06	1.84±.02	2.84±.16	1.45±.01
25	2.96±.31	2.00±.13	3.01±.94	1.75±.35	2.58±.51	1.32±.11
25D	3.01±.06	2.02±.02	3.49±.59	2.05±.19	2.84±.35	1.43±.04
26*	3.33±.22	2.15±.09	2.99±.45	1.76±.15	2.61±.36	1.35±.08
26D*	3.36±.08	2.16±.03	3.19±.30	1.88±.09	2.79±.24	1.44±.02

[1] First parameter set calculated between each data set.

[2] Second decade parameter set (marked D) calculated between each tenth data set.
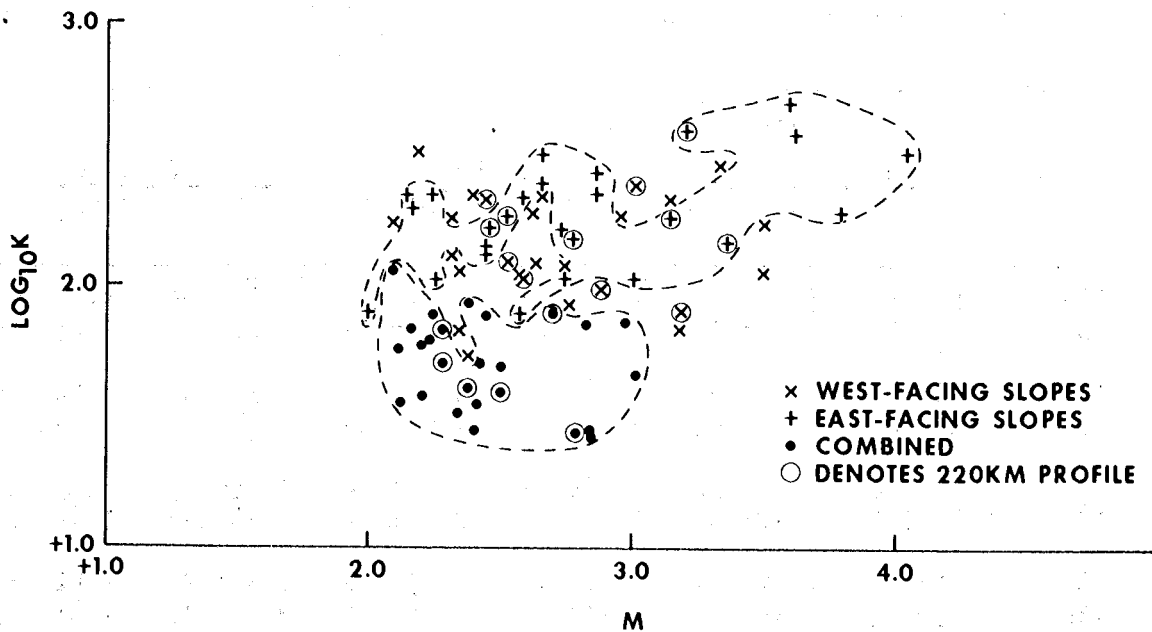
Figure 30. Weighted mean decade parameters m and $\log_{10}k$, South Pacific, using relative frequency. Parameters for 220-km profiles are circled. See also figure 31.

Assuming that theoretical equations (10) and (11) apply, the theoretical constants n and a for the profiles have been calculated (table 14, fig. 32) from weighted decade parameters m and $\log_{10}k$ (table 13, figs. 30 and 31). For values of m near 2, n is zero, the errors in n are large, and the slope frequency is like "white noise" with little tendency to lessen with steepening slope. As the value of m increases, n increases, the errors in n rapidly decrease, and the slope frequency shows an increasingly strong tendency to lessen with steepening slope.

6. DISCUSSION

A straight cumulative plot requires certain stringent requirements in the slope frequency distribution that must be fulfilled by nature and are not due to plotting and sampling methods. The North Pacific profiles will be used as examples. For instance, the natural frequency component of zero slope must be present or else the plots are no longer straight. Also, the natural frequency minimum at 25 m/km (15 fm/interval) on the natural plots (fig. 15) is a character present in at least some, perhaps all, straight cumulative plots. This minimum exists in the natural plots due to natural causes and not just to the methods used. The straight log-log cumulative plot requires a complex interaction between the slope frequency components because of the exponential nature of the relationships.
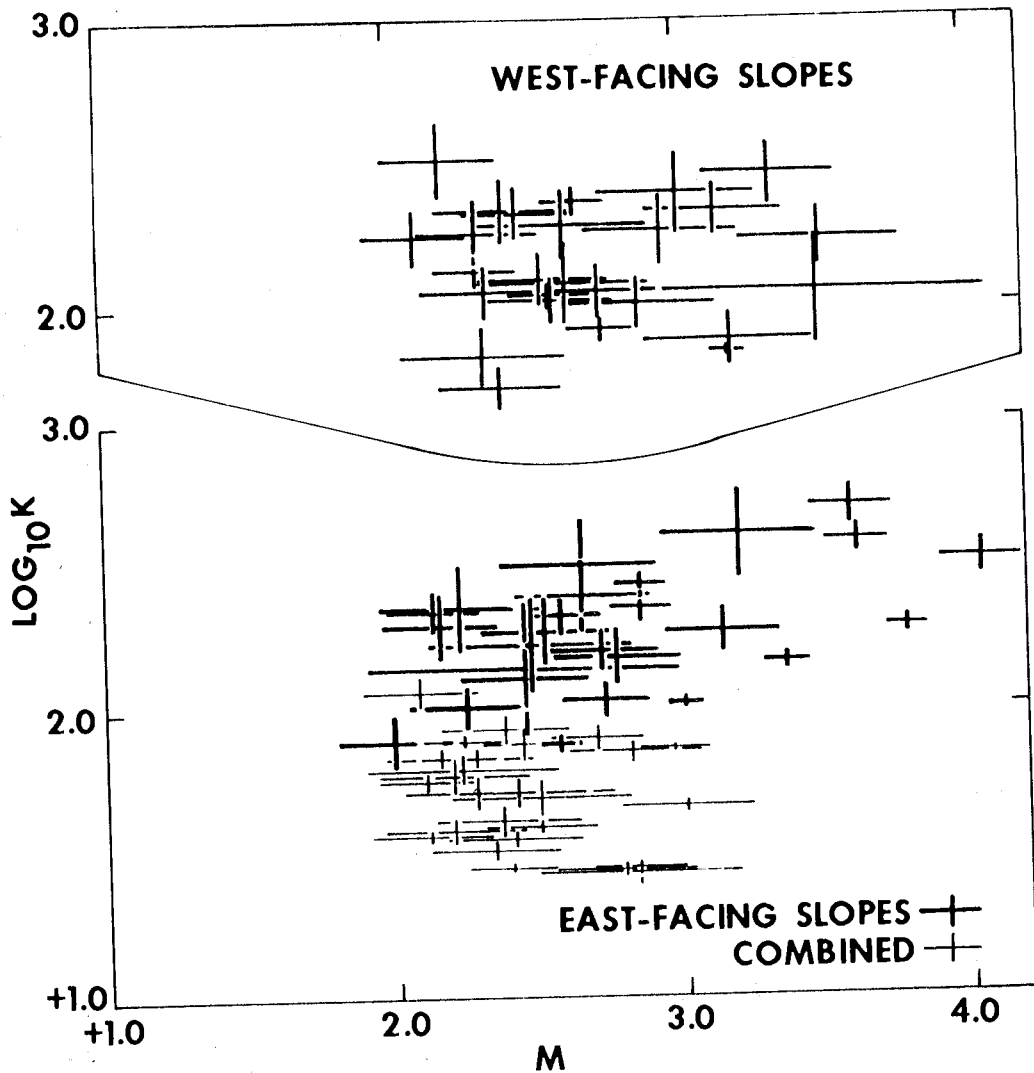
Figure 31. Parameters m and $log_{10}k$ of figure 30 with bars showing weighted standard deviations.

If the cumulative plot is to be straight, each successive slope frequency must be a function of the frequencies of the preceding slope classes. Thus, in theory, the frequency of zero slope can be shown to be very important to the necessary frequencies of the succeeding slope classes required for a straight plot. This is also true for the natural distributions — if the frequency component of zero slope is eliminated, the plots are no longer straight, indicating that nature indeed approaches the ideal. Furthermore, the straight plot also requires an ever-decreasing frequency of successively steeper sea-floor slopes, again a phenomenon inherent in nature as shown in figures 15 through 20. The straight cumulative plot may be taken as an empirical ideal toward which the natural distribution of sea-floor slopes approaches when plotted cumulatively.

Table 14. *Theoretical Parameters n and a Calculated from Mean Decade Parameters m and $\log_{10}k$ of Table 13.*

| Profile | Type of Bottom Slope Compilation | | | | | |
| | East-Facing | | West-Facing | | Combined | |
	n	a	n	a	n	a
1	.12	.004	.16	.003	.08	.006
2	.46	.017	.28	.022	.25	.030
3	.61	.021	.53	.022	.29	.030
4	.19	.005	.24	.010	.14	.012
5	.20	.010	.24	.008	.10	.012
6	.00	.006	.38	.018	.17	.021
7	.42	.022	.42	.021	.29	.030
8	.46	.015	.36	.017	.30	.024
9*	.44	.019	.36	.018	.27	.026
10	.31	.013	.25	.017	.11	.018
11	.67	.031	.60	.031	.50	.043
12*	.53	.024	.46	.026	.33	.032
13	.42	.017	.49	.020	.33	.027
14	.14	.005	.25	.012	.17	.014
15*	.34	.012	.35	.015	.22	.019
16	.36	.022	.42	.025	.29	.035
17	.37	.012	.09	.004	.19	.013
18	.39	.012	.39	.012	.31	.018
19	.31	.012	.29	.008	.19	.015
20*	.32	.011	.31	.009	.22	.015
21	.62	.024	.57	.023	.49	.033
22	.39	.010	.38	.013	.28	.015
23*	.55	.018	.50	.019	.41	.025
24	.64	.034	.54	.039	.46	.050
25	.50	.028	.60	.036	.46	.052
26*	.58	.031	.54	.037	.44	.049

$$S^n \cdot f = a$$

× WEST-FACING SLOPES
+ EAST-FACING SLOPES
○ COMBINED
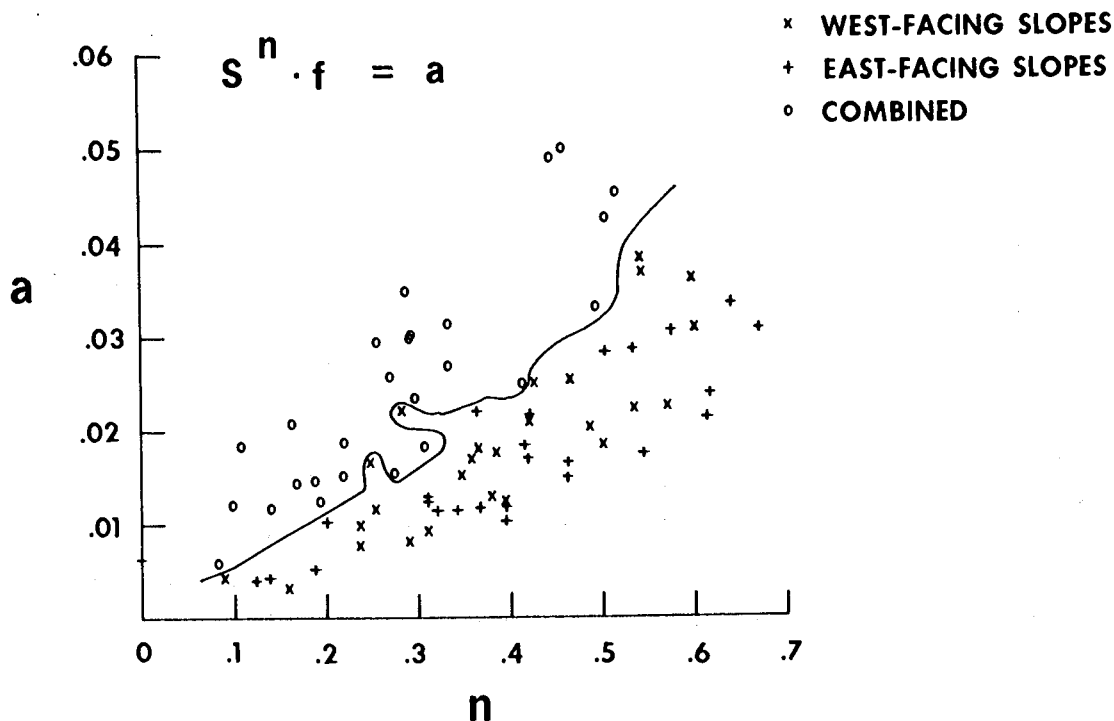
Figure 32. Theoretical parameters n and a, South Pacific, calculated from parameters m and $log_{10}k$ of figures 30 and 31.

All the slope frequency plots in the North Pacific study are compiled in a single graph (fig. 33). These represent all the slopes in all the profiles. Although the distance interval is not the same in all of the profiles, most of them are similar enough so that the main character-istics of the curve are not affected. Also plotted is the cumulative elevation distribution of the slopes. This cumulative distribution is plotted with and without profile 15, which is aberrant compared with the others because it is dominated by a different geologic process: turbid-ity current deposition. The two cumulative curves are similar. The same is done for the frequency distribution, but here the preponderance of flat slopes of profile 15 overweighs the sample so that profile 15 is ignored for the next step.

In a sine curve, flat slopes appear one-half as often as any other slope. An inspection of figure 33 reveals a similar character. This is presented by plotting one-half the frequency of every slope except zero slope, neglecting profile 15. The cumulative elevation plot is adjusted for this by doubling the number of zero slopes. This change straightens the cumulative plot. Therefore, the amount of the zero slope is impor-tant in considering the evolution of the sea-floor morphology.
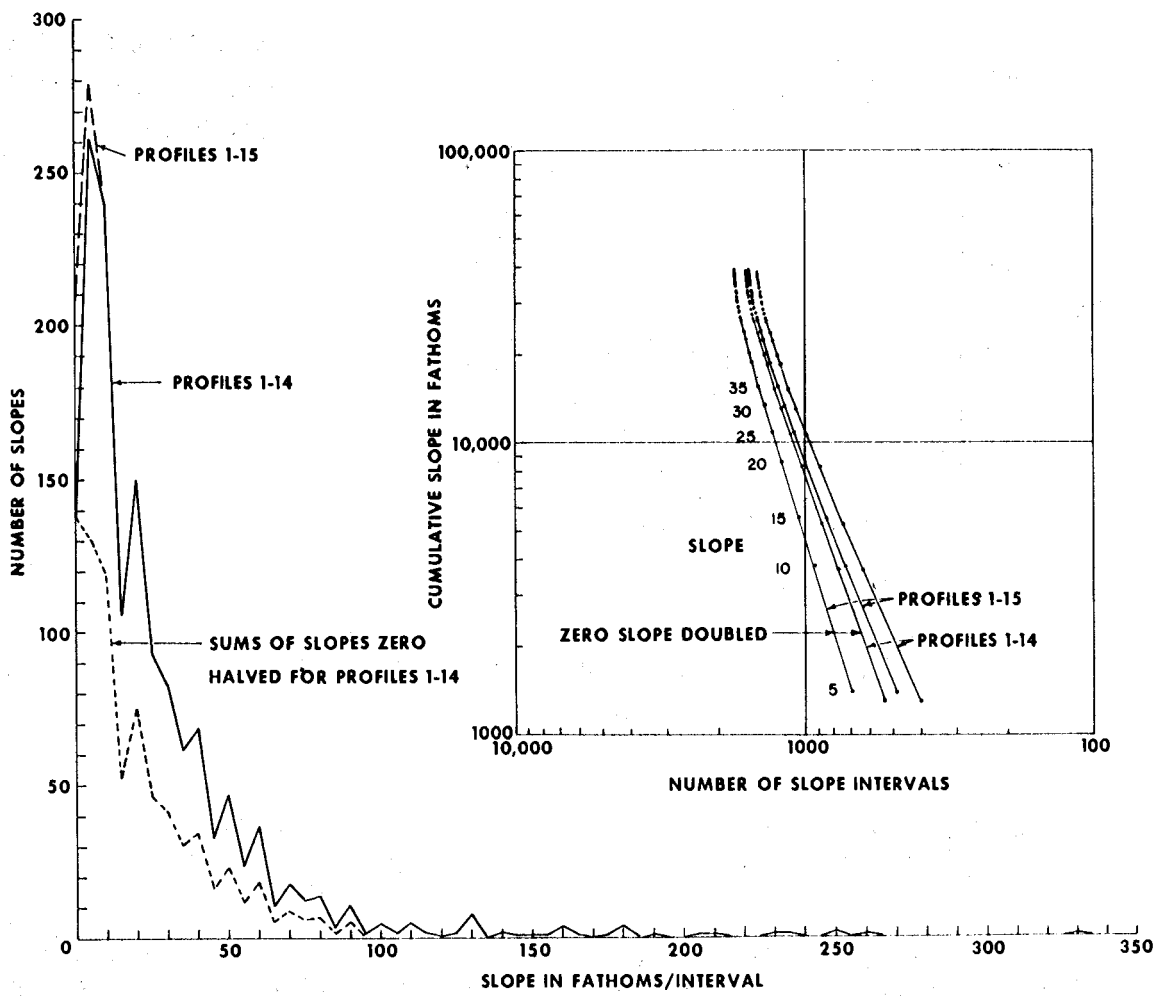
Figure 33. Slope distributions of 15 combined profiles, North Pacific.

7. CONCLUSIONS

7.1 Cumulative Distribution of Slopes

We have demonstrated that slope cumulative distribution in the South Pacific and North Pacific has the form

$$y = kx^m . \tag{18}$$

This has the same form as that of our conceptual model

$$y = \frac{a}{2-n} \left(\frac{1-n}{a}\right)^{\frac{2-n}{1-n}} x^{\frac{2-n}{1-n}} \qquad (6)$$

Therefore, we infer that the valid working hypothesis for the frequency distribution of bottom slopes in the Pacific is

$$s^n f = a \qquad (1)$$

where s is the slope, f is the relative frequency of that slope, a is a parameter, and from (9) $n = \frac{m-2}{m-1}$. Parameter m varies from 2 to 4 (table 13, figs. 30 and 31). Therefore exponent n varies from 0 to 2/3 (table 14, fig. 32), so that from (1) and (10):

1. for m = 2, f = a and k = 1/2a
2. for m = 3, $s^{\frac{1}{2}} f = a$ and $k = 1/12a^2$
3. for m = 4, $s^{2/3} f = a$ and $k = 1/108a^3$

Obviously the value of n can never be greater than 1. The working hypothesis states that the frequency distribution of Pacific bottom slopes is an inverse exponential function of their actual slope.

This exponential-function distribution law is an example of universal law dealing with such diverse phenomena as speech (Mandelbrot, 1953), craters (Baldwin, 1963), and streams (Horton, 1945). These laws have been intensely studied and deal with the so-called rank and size relations (see for example, Rapoport, 1968, Simon, 1955; Mandelbrot, 1953). Our study is not in terms of rank but is similar enough to show similar characters (i.e., decreasing frequency with increasing slope). As Rapoport (1968, p. 321) states, explanations "...are to be sought in the statistical structure of the events that might generate these relations instead of the objects to which the relations apply."

Thus the steeper the slope, the less likely is its occurrence. More important is the law of gravity: the steeper slope is liable to distruction and transformation to a lower slope.

7.2 Geological Relations

The minimum in the North Pacific slope frequency distribution at 1.5° slope and the maximum at 2.0° slope represent a geologic discontinuity on the sea floor. Our interpretation of this feature is that it represents a discontinuity in the sedimentary regime, perhaps between slumps and pelagic sediments.

Summing for all profiles, the cumulative distribution curve for the North Pacific (fig. 33) with doubled-zero slope breaks into three straight lines that probably have geologic significance. The two breaks are at about 3.5° and about 7.5°. The steeper slopes are mostly volcanic rock. The gentler slopes are composed of unconsolidated sediment including the rather fluid sediment noted above. The slopes of 3.5 to 7.5° are typically composed of stiff older sediments or exposed by slumping and/or deformation. Arguing from a very different basis concerning echograms from the Kara Sea, Martynov (1958) came to very similar conclusions regarding stability of the sea-floor sediments.

The foregoing is somewhat less true of the South Pacific where sediment is not as thick. By inference, the breaks in the South Pacific frequency distribution are less pronounced, because of the lack of thick sediment.

For analyses of the hill distribution of the North Pacific profiles see Krause and Menard (1965).

It is suggested that with each class of sediment or rock a log-normal distribution of slopes exists (Micheal Woldenberg, 1971, personal communication). Woldenberg points out that log-normal distributions consist of many random proportionate (i.e., log) variations from a mean rather than random arithmetic variations. The slope frequency distributions (figs. 15, 16 through 20, and 30) appear to be a collection of two (or three) log-normal distributions representing sediment, hard basaltic flows, and tectonism (faulting, slumping associated with faulting, tilting of blocks, etc.) These observations can be regarded as either: (1) a means of explaining the foregoing exponential frequency model, or (2) a separate alternative working hypothesis that remains to be tested.

The hypothesis of the asymmetrical nature of abyssal hills (steeper toward rift) can be tested. Most of the decade parameters m and $\log_{10}k$ have a lower value for the inferred steep direction than for the inferred gentle slope direction, but the results are far from uniform. Of much greater significance, the standard deviations of the decade parameters are usually larger for the inferred steep direction.

By hypothesis, the gentler slopes of the abyssal hills are constructional lava forms. Their low standard deviation implies that the hypothetic magmatic processes closely respond to natural laws, principally gravity. In contrast, the steep sides are more chaotic and by inference the processes — like fault scarp formation — respond poorly to the power laws.

Note that the standard deviations of profiles 24, 25, and 26* are very small, and that parameter m is high. These profiles are inferred to have considerable sediment. Hence, we infer that sedimentation responds to important power-law processes (i.e., gravity).

The consistency of the results indicates that geological complexities, such as difference in spreading rates and nearness of the South Pacific sea floor to a triple junction, do not affect the general laws derived from this study. In contrast, as we learn more about the statistical properties of the profiles, we may be able to quantify those complexities.

Our conclusion is that generalized processes exist that control the geomorphology of the entire East Pacific Rise in very specific and unified ways — thus yielding geomorphic "laws" that control marine geomorphology.

8. SUMMARY

Studies in quantitative marine geomorphology not only yield quantitative measures for classification but also reveal natural geologic laws when unexpected regularities are found. Bathymetric profiles have been intensively examined by quantitative methods in the Northeastern Pacific and South Pacific Ocean, in both cases on the East Pacific Rise. Most of the profiles are 111 km long (60 n miles). The remaining profiles are 222 km (120 n miles) long for comparison. The South Pacific study was a test of quantitative geomorphic relationships found in the North Pacific. Because the two studies cross the same huge tectonic feature, the East Pacific Rise, the studies are considered to be valid for most of the Pacific; most of the Pacific sea floor was formed at the East Pacific Rise or very similar rises. The sea floor is formed at the rift of a rise through a combination of volcanism and tectonism (faulting, slumping, tilting, etc.), and is modified through later sedimentation. The test has been successful.

The depths of the sea-floor profiles are shown to be characterized by a normal distribution or its skewed equivalent, a log-normal distribution. Although most of the depth distributions are unimodal, two or more modes are not unusual, especially for the longer profiles.

The slope frequency distributions are shown to be consistent between the two Pacific studies, but they are not strongly normal as originally thought. The slope distribution is better described as log-normal or as an exponential function. Most importantly, the plots of cumulative slope percent frequency (x) versus cumulative slope (y) are confirmed to show a very strong linearity. This supported the selection of characteristic parameter sets m and $\log_{10} k$ where

$$y = k\,x^m \tag{18}$$

or

$$\log_{10} y = m \cdot \log_{10} x + \log_{10} k \tag{19}$$

Furthermore, parameters m and $\log_{10}k$ are dependent variables for x in percent frequency. For instance, a plot of parameters for all of the profiles yielded the following relations where the parameters represented all of the slopes of a given profile:

North Pacific:

$$m = -0.43 \log_{10} k + 1.8 \tag{27}$$

South Pacific:

$$m = -0.47 \log_{10} k + 1.9 \;. \tag{28}$$

Thus, most of the slopes of any profile or region could be characterized by a single parameter, m. The steeper slopes are not so characterized. For x in *relative* frequency rather than percent, parameter $\log_{10}k$ has a much smaller standard deviation and is relatively independent of parameter m. Hence, relative frequency is preferred.

The cumulative relations of (18) above have the same form as an equivalent equation derived from a conceptual model

$$s^n f = a \tag{1}$$

where s is the slope in m/km, f is the slope's frequency, and n and a are parameters. The results of this paper demonstrate that (1) is the appropriate working model for bottom slope distribution and that n varies from zero to one. That is, the slope frequencies are inversely proportional to a power function of the slope itself.

The linear relationships are a function of the geological processes. The results require that the geological processes produce log-normal effects. Such processes include volcanism, tectonism (and slumping), and sedimentation.

The slope relations in the longer (222-km) profiles are similar to those of the shorter (111-km) profiles. This is not true for depths. The shorter profiles were selected as showing more "uniform" bathymetry than the longer ones, a selection confirmed by the statistical measures. The results suggest the following conclusions: (1) the slope relationships are independent of length of the profile, but (2) the depth relationships yield best results where single geomorphic provinces exist, a distance on the order of 100 km.

9. ACKNOWLEDGEMENTS

10. REFERENCES

Agapova, G. P. (1965): Quantitative characteristics of bottom slope angles in seas and oceans, *Oceanology*, 5(4), 135-138.

Atwater, T. (1970): Implications of plate tectonics for the Cenozoic tectonic evolution of western North America, *Geol. Soc. Amer.*, *81*, 3513-3536.

Atwater, T., and H. W. Menard (1970): Magnetic lineations in the northeast Pacific, *Earth and Planet. Sci. Lett.*, *7*, 445-450.

Atwater, T. M., and J. D. Mudie (1968): Block faulting on the Gorda Rise, *Science*, *159*, 729-731.

Baldwin, R. B. (1963): *The Measure of the Moon* (Univ. of Chicago Press, Chicago), 488 p.

Barazangi, M., and J. Dorman (1968): World seismicity map of ESSA Coast and Geodetic epicenter data for 1961-1967, *Seismol. Soc. Amer. Bull.*, *58*, 369-38.

Engel, A. E. J., and C. G. Engel (1964): Composition of basalts from the Mid-Atlantic Ridge, *Science*, *144*, 1330-1333.

ESSA (1970): *World Seismicity, Mercator Chart NEIC-3005* (U. S. Coast and Geodetic Survey, Washington, D. C.).

Ewing, J., and M. Ewing (1967): Sediment distribution on the mid-ocean ridges, *Science*, *156*, 1590-1592.

Goldberg, E. D., and M. Koide (1962): Geochronological studies of deep sea sediments by ionium/thorium method, *Geochim. Cosmochim. Acta*, *26*, 417-450.

Hayes, D. E., J. R. Heirtzler, E. M. Herron, and W. C. Pitman III (1969): Preliminary report of Volume 21, U.S.N.S. *Eltanin*, Cruises 22-27, January 1966-February 1967, Part A and Part B, Tech. Rept. No. 2-CU-2-69, Lamont-Doherty Geol. Obs. (Columbia Univ.), p. 99.

Hayes, D. E., M. Talwani, R. Houtz, W. C. Pitman III, and R. R. Meijer II, (1972): Preliminary report of Volume 22, U.S.N.S. *Eltanin* Cruises 28-32, March 1967-March 1968, Tech. Rept. No. CU-1-72, Lamont-Doherty Geol. Obs (Columbia Univ.) 232 pp.

Heezen, B. C., and T. L. Holcombe (1965): Geographic distribution of bottom roughness in the North Atlantic, Bell Telelphone Labs, Inc., and Lamont-Doherty Geol. Obs. (Columbia Univ, Palisades, N.Y.), 41 pp. and 6 charts.

Heirtzler, J. R., G. O. Dickson, E. M. Herron, W. C. Pitman III, and
     X. Le Pichon (1968): Marine magnetic anomalies, geomagnetic field
     reversals, and motions of the sea floor and continents, *Jour.
     Geophys. Res., 73*, 2119-2136.

Herron, E. M. (1971): "Crustal plates and sea floor spreading in the
     southeastern Pacific." Amer. Geophys. Un., *Antarctic Oceanology I,
     Antarctic Res. Ser., 15*, 229-237.

Herron, E. M. (1972): Sea floor spreading and the Cenozoic history of
     the east-central Pacific, *Geol. Soc. Amer. Bull., 83*, 1671-1692.

Herron, E. M., and D. E. Hayes (1969): A geophysical study of the Chile
     ridge, *Earth and Planet. Sci. Lett., 6*, 77-83.

Hoffman, J. (1957): Hyperbolic curves applied to echo sounding, *Intern.
     Hydrographic Rev., 34*(2), 45-55.

Holcombe, T. L., and B. C. Heezen (1970): Patterns of relative relief,
     slope and topographic texture in the North Atlantic Ocean, Lamont-
     Doherty Geol. Obs., Tech. Rept. No. 8 (Columbia Univ., Palisades,
     N. Y.), 127 pp. and 6 charts.

Horton, R. E. (1945): Erosional development of streams and their drainage
     basins: hydrophysical approach to quantitative morphology, *Geol.
     Soc. America Bull., 56*, 275-370.

Keller, G. H., and G. Peter (1968): East-west profile from Kermadec
     trench to Valparaiso, Chile, *Jour. Geophys. Res., 73*(22), 7154-
     7157.

Krause, D. C. (1962): Interpretation of echo sounding profiles, *Inter.
     Hydrographic Rev., 39*(1), 65-123.

Krause, D. C., and H. W. Menard (1965): Depth distribution and bathy-
     metric classification of some sea floor profiles, *Marine Geology,
     3*, 169-193.

Krause, D. C., and V. F. Kanaev (1970): Narrow beam echo sounding in
     marine geomorphology, *Inter Hydrographic Rev., 48*(1), 23-33.

Krumbein, W. C., and F. A. Graybill (1965): *An Introduction to Statis-
     tical Models in Geology* (McGraw-Hill Book Co., New York), 475 pp.

Larson, R. L., and F. N. Spiess (1970): Slope distributions of the East
     Pacific Rise crest, SIO Ref. 70-8 (Scripps Inst. Ocean., Univ.
     California, San Diego), 4 pp.

Le Pichon, X. (1968): Sea floor spreading and continental drift, *Jour.
     Geophys. Res., 73*, 3661-3697.

Loughridge, M. S., and F. N. Spress (1968): Abyssal hill slope distributions and sonar bearing errors, Scripps Inst. Ocean. (Univ. California, San Diego), SIO Ref. 68-44, 5 pp.

Mandelbrot, B. (1953): "An informational theory of the statistical structure of language." *Communication Theory*, ed. by W. Jackson, 486-502 (Academic Press, New York), 603 pp.

Martynov, V. T. (1958): The appearance of underwater landslides on the echo tape, *Problemy Arktiki*, *3*, 95-101, Translation by R. Flagg, Amer. Meteorological Soc. (Defense Documentation Ctr., Cameron Station, Alexandria, Va.), as FR-280, 11 pp.

Matthews, D. J. (1939): Tables of the velocity of sound in pure water and sea water for use in echo-sounding and sound-ranging, Admiralty Hydrographic Dept., London, Pub. H.D. 282, 52 pp.

McConnell, R. K., Jr. (1967): "Dike propagation." *Economic Geology in Massachusetts*, ed. by O. C. Farquhar, 97-104 (Univ. Mass. Grad. School), 1967.

McDonald, M. F., and E. J. Katz (1969): Quantitative method for describing the regional topography of the ocean floor, *Jour. Geophys. Res.*, *74*(10), 2597-2607.

McDonald, M. F., E. J. Katz, and R. W. Faas (1966): Depth study report on the detectibility of submarines on the ocean bottom, Vol. III, Electric Boat Div. (Gen. Dynamics Corp., Groton, Conn.), Rept. U413-66-116.

McKenzie, D. P., and J. G. Sclater (1969): Heat flow in the eastern Pacific and sea floor spreading, *Bull. Volcanol.*, *33*(1), 101-118.

Morgan, W. J., P. R. Vogt, and D. F. Falls (1969): Magnetic anomalies and sea floor spreading on the Chile rise, *Nature*, *222*(5189), 137-142.

Northrup, J. (1972): Seismicity gaps in the Pacific Antarctic Ridge and East Pacific Rise, Inter. Sym. of Oceanography in So. Pacific, New Zealand Nat. Comm. for UNESCO, Wellington, Abstracts, p. 92.

Papopart, A. (1968): "Rank-size relations." *Inter. Encyclopedia of the Social Sciences*, *13*, 316-323 (Crowell Collier and McMillan Inc.).

Sclater, J. G., and J. Francheteau (1970): The implications of terrestrial heat flow observations on current tectonic and geochemical models of the crust and upper mantle of the earth, *Geophys. J. Roy. Astron. Soc.*, *20*, 509-542.

Schlater, J. G., R. N. Anderson, and M. L. Bell (1971): Elevation of ridges and evolution of the central eastern Pacific, *Jour. Geophys. Res., 76*(32), 7888-7915.

Simon, H. A. (1955): On a class of skew distribution functions, *Biometrika, 42,* 425-440.

Smith, F. G. (1966): *Geological Data Processing Using FORTRAN IV* (Harper and Row Pub., N. Y.), 284 pp.

Smith S. M., T. E. Chase, W. E. Farrell, I. L. Taylor, and M. E. Weed (1965): Distribution and statistical analysis of sea floor relief in the northeast Pacific, Bell Telphone Labs and Univ. of Calif. at San Diego, Tech. Rept. 6-601347, 59 pp. and 8 charts.

Spiess, F. N. B. Luyendyk, and M. S. Loughridge (1969): Bottom slope distributions and implied acoustic bearing errors in abyssal hill regions of the North Pacific, *Jour. Underwater Acous. (USN), 19*(2), 183-196.

Switzer, P., C. M. Mohr, and R. E. Heitman (1964): Statistical analyses of ocean terrain and contour plotting procedures (Arthur D. Little, Inc., Cambridge, Mass.), Rept. No. 1440464 (AD 601538), 75 pp.

Szekely, J., and P. H. Reitan (1971): Dike filling by magma intrusion and by explosive entrainment of fragments, *Jour. Geophys. Res., 76*(11), 2602-2609.

Tyler, G. L., and R. A. Simpson (1970): Bistatic radar measurements of topographic variations in lunar surface slopes with Explorer 35, *Radio Science, 5*(2), 263-271.

Tyler, G. L., R. A. Simpson, and Henry J. Moore (1971): Lunar slope determinations: comparison of bistatic-radar and photographic results, *Jour. Geophys. Res., 76*(11), 2790-2795.

Vine, F. J. (1966): Spreading of the ocean floor — new evidence, *Science, 154,* 1405-1415.

Vogt, P. R., E. D. Schneider, and L. G. Johnson (1969): The crust and upper mantle beneath the sea, *Amer. Geophys. Un., Geophys. Mono., 13,* 556-617.